

Article

Hydrodynamics of Collapsing Glass Tubes and Measuring of Glass Viscosities: Analytic Results beyond Asymptotic Approaches for Rapidly Varying Viscosities

Thomas Klupsch 

Independent Researcher, Mädertal 4, D 07745 Jena, Germany; thomas.klupsch@t-online.de

Abstract: We present novel analytic solutions of the axial-symmetric boundary value problem of the Stokes equation for incompressible liquids with rapidly varying viscosity, which cover the hydrodynamics of collapsing glass tubes with moving torch. We meet requirements to optimize the contactless measuring of dynamical viscosities and surface tensions of molten glasses through collapsing for tools working with sharply peaked axial temperature courses. We study model solutions for axial courses of the reciprocal viscosity specified as Gaussians extended on small distances compared to the outer tube radius, and we neglect the boundary inclination, corresponding to measuring conditions for large torch velocities. The surface tension is assumed to be constant across the collapsing zone. The boundary value problem becomes disentangled, changing to a gradually independent hierarchy of streaming function, vorticity, and pressure. Axial Fourier transforms are introduced to focus on solutions for infinitely extended tubes. Beyond the predictions of the asymptotic collapsing theory, a successively increasing steepness of the reciprocal viscosity induces an increasing radial pressure gradient that acts against the surface tension and diminishes the collapsing efficiency. The arising systematic error in evaluating the viscosity from experimental data in virtue of the asymptotic collapsing theory is corrected. Error estimations regarding deviations from the specified viscosity course, the neglected boundary inclination, and heat conduction within the tube wall are outlined, and preconditions to simplify the measuring of surface tensions through collapsing are discussed.

Keywords: highly viscous fluids; molten glasses; contactless viscosity measuring; surface tension; collapsing of glass tubes; Stokes equation with free boundaries; rapidly varying viscosity; viscous flow and vorticity



Citation: Klupsch, T. Hydrodynamics of Collapsing Glass Tubes and Measuring of Glass Viscosities: Analytic Results beyond Asymptotic Approaches for Rapidly Varying Viscosities. *Fluids* **2021**, *6*, 179. <https://doi.org/10.3390/fluids6050179>

Academic Editor: Antonio Santamaría

Received: 11 March 2021

Accepted: 27 April 2021

Published: 6 May 2021

Publisher's Note: MDPI stays neutral with regard to jurisdictional claims in published maps and institutional affiliations.



Copyright: © 2021 by the author. Licensee MDPI, Basel, Switzerland. This article is an open access article distributed under the terms and conditions of the Creative Commons Attribution (CC BY) license (<https://creativecommons.org/licenses/by/4.0/>).

1. Introduction

This work is interdisciplinary. It may contribute to the theoretical base to establish collapsing of glass tubes as a precise, contact-free method to measure temperature-dependent viscosities [1–11] and surface tensions [9,10] of molten glasses. There is a general consensus that molten glasses should be treated as highly viscous Newtonian fluids. This shows that exclusively laminar flow can occur. Our work may also contribute to succeed in the analytic treatment of boundary value problems of the Stokes equation, in particular, if the viscosity rapidly varies on length scales of the confinement, so that asymptotic methods [11] fail.

When an axial section of a glass tube is heated such that the glass becomes a viscous fluid, the tube will collapse back upon itself inside the heating zone, driven by the surface tension. We will focus here on collapsing under steady-state conditions only, and the term “collapsing” will be exclusively used for steady-state collapsing. This occurs if the heat source moves uniformly along the tube. Then an observer comoving with the heat source becomes aware of a steady-state collapsing profile narrowed against the direction of motion. It is provided, of course, that the comoving observer measures, at the same time, an accompanying steady-state temperature field. If, in addition, different axial streaming

velocities are impressed on both sides of the heating zone such that the impressed flow difference will play the role of the proper driving force, one speaks of “drawing”.

Collapsing and drawing are known, first at all, as fundamental technology steps in the fabrication of optical fibers and complex fiber structures (for a survey on theoretical problems in the area of collapsing, see, e.g., [2,9,11], and drawing, see, e.g., [12–17]). The principle of collapsing is also applied to the so-called redraw process to produce highly precise glass sheets for optical applications (see, e.g., [18,19]). In our work, we focus on preferably simple arrangements where a comprehensive understanding of all aspects of collapsing is essential. The horizontal collapsing arrangement studied here is sketched in Figure 1. It is the same as investigated in [11].

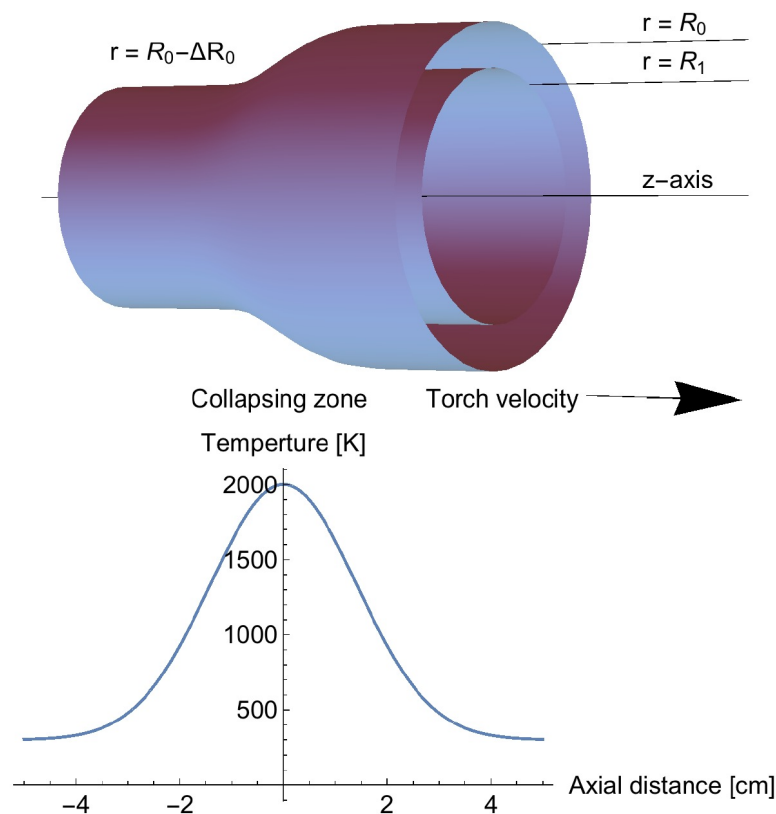


Figure 1. Schematic plot of steady-state collapsing of a glass tube, shown from the perspective of an observer comoving with the torch. The comoving collapsing tube profile is depicted versus the characteristic comoving steady-state axial course of the tube temperature. The torch velocity, measured in the labor frame, is directed against the reduction of the tube radii.

The glass tube may be fixed in the labor frame. The tube wall may be represented by two infinitely extended circular, coaxial cylinders. A mobile heat source (simply called “torch” in the following) may move along the tube with uniform velocity and create, steady-state conditions provided, a comoving steady-state peak of the tube temperature. If the maximum temperature is large enough so that the glass becomes a viscous fluid, the surface tension induces a radial force towards the cylinder axis. Then the moving torch becomes accompanied by a comoving cone-like reduction of the tube dimensions against the moving direction (see Figure 1). To determine the temperature-dependent dynamical glass viscosity (simply called “viscosity” in the following), the input data from steady-state collapsing measurements are the tube radii and tube wall thickness, respectively, before collapsing, the torch velocity, and the reduction of the outer tube radius and increasing of the wall thickness, respectively, after collapsing. These data are supplied by the current axial course of the tube temperature. All input data can be precisely determined with the aid of optical and pyrometric tools, respectively (not shown in Figure 1). For details, see, e.g., [9,10].

For perpendicularly arranged drawing equipment, contactless, non-steady-state in situ viscosity measurements on compact glass fibers have been described (for a recent version, see, e.g., [20]). The measuring principle exploits the time-dependent fiber elongation around a temperature hot spot where the glass becomes a highly viscose fluid and the balance between gravity and resetting force through surface tension is slightly disturbed. The surface tension by itself is determined from the force equilibrium conditions. A strong hydrodynamic analysis is not known so far.

The steady-state viscosity measurement through collapsing requires the knowledge of any ad hoc model relations describing the general temperature dependence of the viscosity for selected material classes. This approach is necessary to determine, by calculation only, that axial viscosity course which correlates with the measured axial temperature course. More precisely, the measurement of the temperature-dependent glass viscosity through collapsing comprises the determination of two or more parameters involved in such ad hoc model relations, e.g., the Arrhenius law and the Vogel-Fulcher law with two and three parameters, respectively (for details, see, e.g., [21]). Assuming, for a moment, these parameters are known, the precise axial viscosity course is known, too, and the collapsing theory should be able to verify the measured steady-state collapsing profile. The inverse problem, namely the back-calculation of those parameters in question from experimental data is more complicated and to some degree straightforward only if preconditions are met to use the asymptotic analysis. We refer to Sections 4 and 5. Clearly, the determination of two or more unknown parameters entering formulae of the temperature-dependent viscosity requires two or more independent collapsing measurements. Finally, measurements of the surface tension of molten glasses can be involved into collapsing experiments [9,10]. The idea is, in principle, a modification of the well-known bubble pressure method [22], applied to collapsing equipment. We refer to Section 4.2.

The collapsing theory outlined here as well as in previous papers is based on the Stokes equation for incompressible liquids, regarding the extremely low Reynolds number of molten glasses under collapsing conditions of about 10^{-7} . Initially, very simple mathematical approximations motivated more by physical intuition were used to describe the collapse process [1,2,5–9]. In [11], a comprehensive analysis has been given, applying the ideas of the asymptotic multi scale analysis (AMSA). It is ad hoc provided there that the spatial dependence of hydrodynamic and geometric quantities is governed by different length scales h and l in radial and axial direction, respectively, where $\varepsilon = h/l \ll 1$. As far as this fundamental premise holds true in practice, AMSA considerably facilitates the analysis of collapsing. In particular, it allows an entangled perturbation treatment of hydrodynamic equations, boundary conditions, and kinematics in powers of ε , which is also the base to classify various complex effects contributing to collapsing. h and l naturally stand for the outer tube radius before collapsing, and the axial width of the reciprocal viscosity, respectively, where l is also a measure of the axial width of the temperature peak. In practice, the AMSA in zeroth order dealing with the radial flow component only, and in first order, dealing with both the radial and axial flow component, can be performed with reasonable effort (in [11] denoted as 1D and 2D theory, respectively). The error estimation [11] shows that AMSA becomes successively erroneously for $\varepsilon > 1/2$ where the data evaluation through AMSA becomes questionably.

Unfortunately, the preconditions where AMSA works well do not sufficiently meet two basic experimental requirements to arrive at a highly precise ascertainment of the above-mentioned input data after collapsing. First, the tube radii should be chosen as large as possible (≥ 1 cm) to minimize the error in the optical shrinking measurements [9,10]. Secondly, the exact record of the temperature course requires the entire visibility of the glass tube crossing the heating zone. This latter condition is well satisfied by equipment applying oxyhydrogen ring burners [9,10] which can produce, in addition, rather sharp and well reproducible temperature peaks. But the optimum choice regarding both the preconditions is found for about $1 \leq \varepsilon \leq 3$. Earlier attempts to operate with tube-shaped furnaces where

the collapsing zone is invisible and the peak temperature must be estimated [23] are not helpful, although the axial length of the heating zone could be arbitrarily chosen.

To the authors knowledge, no strong analytical solutions of more complex boundary value problems of the Stokes equation have been published, which could serve as a guide for the problem to be solved here. The general attention regarding variable viscosities seems still focused on finding of rigorous analytical solutions as such in the first place. In this context, the early work of Martin (1971) [24] is still of interest (see, e.g., [25–27]), which exploits a relationship between a variable viscosity and the vorticity. However, completely different methods, e.g., mode coupling [28,29] have been investigated, too, for geophysical applications [29,30], but mainly to find so-called benchmark solutions to adjust computer calculations [30,31].

Thus, our mathematical approach is novel, and without exploiting abstract functional-analytic methods. We present a classical analysis of the hydrodynamics of collapsing without the ad hoc restriction to sufficiently broad peaks of the axial temperature course and reciprocal viscosity, respectively. We focus on model courses of the axially dependent reciprocal viscosity chosen as Gaussians. The Stokes equation with the full set of boundary conditions is solved for infinitely extended tubes with constant radii. This implies the exact description of the collapsing kinematics for the limiting case of large torch velocities. We use the conception of AMSA only for error estimations for more general viscosity courses, as well as for torch velocities below the asymptotic limit. In Section 2, we start with the Stokes equation for incompressible liquids. In particular, we focus on the transformed version for axial symmetry and an axial viscosity dependence outlined in [11], given as coupled equations for the stream function, vorticity and pressure. A program to arrive at a clearly arranged treatment of boundary conditions is carried out in Section 3. The stream function discussed in Section 3.1 is shown to be closely related to the balance of the normal forces on both the surfaces, meanwhile the vorticity analyzed in Section 3.2 is governed through the tangential force balance even there. Both the functions will induce separate, space-dependent contributions to the pressure, discussed in Section 3.3. Because, vice versa, the pressure participates in the normal force balance, an equation to guarantee the self-consistency of all hydrodynamic functions is established and solved in Section 3.4. The collapsing kinematics is discussed in Section 4. We point out that the earlier concise formulae from AMSA for determining of the viscosity from collapsing data must be supplied by a correction factor only, meanwhile the surface tension can be measured through suppression of collapsing, where no knowledge of the viscosity course is required at all. The general discussion in Section 5 is focused on optimized experimental conditions to minimize unavoidable systematic errors in the viscosity measurement.

2. Equations and Boundary Conditions

The collapsing tube walls and the main components of the viscous flow and vorticity are sketched in Figure 2. The axis of the collapsing tube may be the z -axis of a cylinder coordinate system (r, φ, z) . The outer and inner tube radius before collapsing may be denoted by R_0 , and R_1 , respectively.

For incompressible fluids, the Stokes equations read

$$\eta \Delta \mathbf{v} + \sigma' \cdot \nabla \eta = \nabla \cdot p, \quad (1)$$

$$\nabla \cdot \mathbf{v} = 0. \quad (2)$$

\mathbf{v} is the viscous flow vector, p the pressure inside the tube, η the viscosity, and $\eta \cdot \sigma'$ that part of the stress tensor originated by the viscous material properties. $\mathbf{n}_0, \mathbf{n}_1$, and $\mathbf{t}_0, \mathbf{t}_1$ denote the normal and tangential vector at the outer and inner tube surface, respectively. We will focus on the analysis of the viscous flow field if the outer and inner tube radius can be provided as constant, i.e., independent of z (see Sections 4 and 5 for a detailed

discussion). Then the flow field is determined as solution of (1) and (2) with the boundary conditions (see, e.g., [11])

$$\mathbf{n}_i \cdot (p - \eta \sigma') \cdot \mathbf{n}_i = (-1)^i \cdot \tau / R_i, \quad i = 0, 1, \tag{3}$$

$$\mathbf{t}_i \cdot \sigma' \cdot \mathbf{n}_i = 0, \quad i = 0, 1, \tag{4}$$

where (3) and (4) is the balance condition of the normal and tangential force on both the tube surfaces, respectively. τ is the surface tension, which is assumed to be constant (see also Section 4.2). We will denote (3) and (4) as the radial boundary conditions. The latter must be supplied by axial boundary conditions. In what follows, we will consider an infinitely extended tube where away from the heating zone, the viscosity continuously but unlimited increases so that the viscous flow driven by limited external forces must expire. Thus, we have the axial boundary condition

$$\mathbf{v} \rightarrow 0, \quad \text{if } z \rightarrow \pm\infty. \tag{5}$$

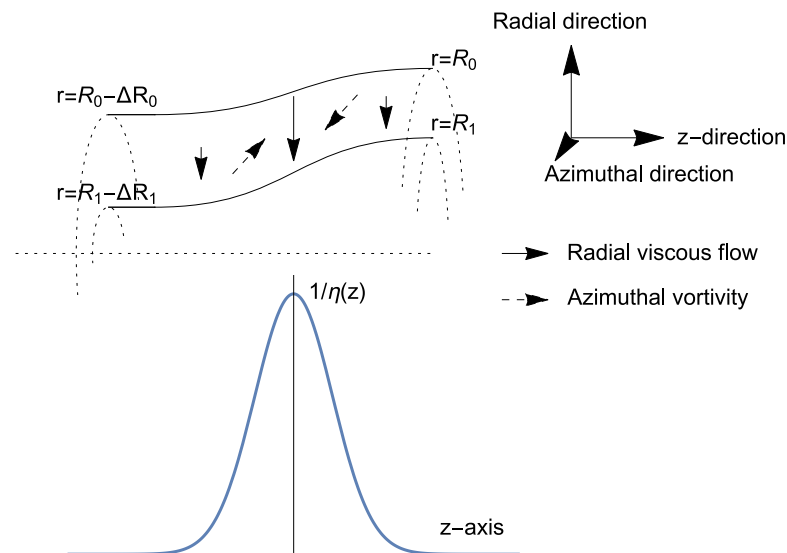


Figure 2. Schematic plot: Snapshot (labor frame) of a (r, z) -cross-sectional area of the tube wall across the collapsing zone, versus axial course of the reciprocal viscosity. Solid arrows: the main (radial) viscous flow component. Dotted arrows: the exclusively azimuthally directed vorticity vector.

The torch may move along the tube with the constant velocity v_T in $+z$ -direction. We will restrict to steady-state conditions, i.e., an observer which comoves with the torch may measure steady-state quantities in his frame of reference. In particular, we will assume a model viscosity course, which is steady-state in the comoving frame of reference, according to

$$\eta(r, \varphi, z, t) = \eta_{min} \cdot \exp(z'^2 / \Delta z_e^2), \tag{6}$$

$$z' = z - v_T t, \tag{7}$$

where η_{min} and Δz_e denote the minimum viscosity, and the half of the axial width where the viscosity increases to its e -fold minimum value, respectively. The Stokes Equations (1) and (2) and the boundary conditions (3) to (5) are invariant against the transformation (7) from labor coordinates (r, φ, z) to coordinates (r, φ, z') which comove with the torch. Therefore, we will make the agreement to change generally to comoving coordinates, so that an explicit time-dependence disappears in describing the steady state in comoving coordinates. More precisely, the viscous flux and the stress tensor are understood to be measured in the labor

frame, but treated as functions of the comoving coordinates, as with all other hydrodynamic quantities. In the following, z may denote the comoving axial coordinate.

Following [11] we will make the second agreement to change to dimensionless quantities and coordinates so that (1) to (4) remain invariant. Based on three benchmarks Λ (length benchmark), η_{min} , and τ , the dimensionless radial and axial coordinate \bar{r} , and \bar{z} are introduced by $\bar{r} = \Lambda r$, and $\bar{z} = \Lambda z$, respectively, and the velocity v and pressure p in physical units become scaled through the corresponding dimensionless quantities \bar{v} and \bar{p} by $v = (\tau/\eta_{min})\bar{v}$, and $p = (\tau/\Lambda)\bar{p}$, respectively. The dimensionless viscosity $\bar{\eta}$ and surface tension are given by $\bar{\eta} = \eta/\eta_{min}$, and $\bar{\tau} = 1$, respectively. Λ will be chosen as $\Lambda = R_0$. For further details see [11]. All mathematical expressions outlined below will be given in dimensionless units, where we will renounce the overbar (for clearness, the symbol R_0 will be used furthermore). Then the model course of the dimensionless reciprocal viscosity yields

$$1/\eta(z) = \exp(-\alpha^2 z^2), \tag{8}$$

where $\alpha = R_0/\Delta z_e$.

Through the boundary conditions (3), (4) and the precondition (6), our problem becomes an axial-symmetrical one so that all quantities of interest will depend upon r and z only. The further treatment according to [11] aims at the elimination of the inconvenient restriction (2). This is done introducing the vector potential \mathbf{A} according to

$$\mathbf{v}(r, z) = \nabla \times \mathbf{A}(r, z). \tag{9}$$

In cylinder coordinates, \mathbf{A} reads

$$\mathbf{A}(r, z) = \mathbf{e}_\varphi \cdot A_\varphi(r, z), \tag{10}$$

with \mathbf{e}_φ as the azimuthal unit vector. The azimuthal component $A_\varphi(r, z)$ of the vector potential is the stream function of our problem, from which the radial and axial flux component, $v_r(r, z)$ and $v_z(r, z)$, respectively, are derived according to

$$v_r(r, z) = -(\partial/\partial z)A_\varphi(r, z), \tag{11}$$

$$v_z(r, z) = (1/r)(\partial/\partial r)(rA_\varphi(r, z)). \tag{12}$$

It is shown in [11] that, starting from (9), (10), the Stokes Equation (1) can be transformed into three coupled equations for the stream function $A_\varphi(r, z)$, an auxiliary function $Q''(r, z)$, and the pressure $p(r, z)$, according to

$$(\mathcal{D}_r + \partial^2/\partial z^2)A_\varphi(r, z) = Q''(r, z)/\eta(z), \tag{13}$$

$$(\mathcal{D}_r + \partial^2/\partial z^2)Q''(r, z) = 2(d^2\eta(z)/dz^2) \cdot \mathcal{D}_r A_\varphi(r, z), \tag{14}$$

$$(\partial/\partial r)p(r, z) = -(\partial/\partial z)Q''(r, z) + 2(d\eta(z)/dz) \cdot \mathcal{D}_r A_\varphi(r, z), \tag{15}$$

where the operator \mathcal{D}_r stands for

$$\mathcal{D}_r \equiv (\partial/\partial r)(1/r)(\partial/\partial r)r. \tag{16}$$

The auxiliary function $Q''(r, z)$ introduced in [11] guarantees the compatibility of the ansatzes (9), (10) with (1). One can show (the author thanks one of the referees of [11] for this suggestion) that $-Q''(r, z)/\eta(z)$ agrees with the azimuthal component of the vorticity vector $\boldsymbol{\Omega}(r, z) = \nabla \times \mathbf{v}(r, z) = \nabla \times \nabla \times \mathbf{A}(r, z)$. Indeed, evaluating the r. h. s. of the foregoing relation and observing $\nabla \cdot \mathbf{A} = 0$, as concluded from (10), we arrive at $\boldsymbol{\Omega}(r, z) = -\Delta \mathbf{A}(r, z) = -\mathbf{e}_\varphi \cdot (\mathcal{D}_r + \partial^2/\partial z^2)A_\varphi(r, z)$ (see, e.g., [32]), and the argued result follows from (13).

For the remaining of this paper, we abbreviate

$$S(r, z) = Q''(r, z) / \eta(z). \tag{17}$$

$S(r, z)$ will be denoted as the vorticity function, the equation of which is simply found substituting (17) into (14). At this point, we take a step further to circumvent complicated expressions of $\eta(z)$ involved in (14). If we ad hoc commit ourselves to the model course (8) of the reciprocal viscosity, further substitute $\mathcal{D}_r A_\varphi(r, z)$ on the r. h. s. of (14) via (13), and divide by $\eta(z)$, where $\eta(z) \neq 0$, we obtain

$$\begin{aligned} & (\mathcal{D}_r + \partial^2 / \partial z^2 + 4\alpha^2 z \partial / \partial z - 2\alpha^2 - 4\alpha^4 z^2) S(r, z) \\ & = -(4\alpha^2 + 8\alpha^4 z^2) (\partial^2 / \partial z^2) A_\varphi(r, z). \end{aligned} \tag{18}$$

To derive the radial boundary conditions of $A_\varphi(r, z)$ and $S(r, z)$ to be applied in practice we need the following tensor components of σ' (see, e.g., [32])

$$\sigma'_{rr} = 2(\partial / \partial r) v_r(r, z) = -2(\partial^2 / \partial r \partial z) A_\varphi(r, z), \tag{19}$$

$$\sigma'_{rz} = (\partial / \partial z) v_r(r, z) + (\partial / \partial r) v_z(r, z) = (-\partial^2 / \partial z^2 + \mathcal{D}_r) A_\varphi(r, z), \tag{20}$$

to be substituted in (3) and (4), respectively. Because σ' is expressed in terms of the streaming function $A_\varphi(r, z)$ only, apparently, $A_\varphi(r, z)$ would become over-constrained through the four boundary conditions (3), (4) regarding the radial dependence. Indeed, the vorticity function $S(r, z)$ provides the missing degrees of freedom required to satisfy all balance conditions on both the tube boundaries, as seen below.

The pressure $p(r, z)$ is given by the radial integration of (15) up to an arbitrary constant p_0 , as shown in [11]. In what follows, it is very useful to subdivide $p(r, z)$ into a constant and a variable part, p_0 and $\Delta p(r, z)$, respectively, according to

$$p(r, z) = p_0 + \Delta p(r, z), \tag{21}$$

where the radial integration of (15) may be carried out such that

$$\Delta p(R_1, z) = 0. \tag{22}$$

We will call $\Delta p(r, z)$ the variable “hydrodynamic” pressure part, because depending upon the viscous flow only. The boundary condition (3) can be rewritten, taking into account (19):

$$\begin{aligned} & (p_0 + \Delta p(r, z)) \exp(-\alpha^2 z^2) + 2(\partial^2 / \partial r \partial z) A_\varphi(r, z) \\ & = \pm(1/r) \exp(-\alpha^2 z^2), \end{aligned} \tag{23}$$

where the upper and lower sign on the r.h.s. of (23) is valid for $r = R_0$ and $r = R_1$, respectively.

The boundary condition of the tangential force balance (4) will be reformulated to become a boundary condition for the vorticity function. This boundary condition remains dependent upon the stream function. Observing (20) and introducing $S(r, z)$ according to (13) and (17), we get

$$S(r, z) = 2 \mathcal{D}_r A_\varphi(r, z) \text{ at } r = R_0 \text{ and } r = R_1. \tag{24}$$

The reciprocal viscosity $1/\eta(z)$ governs the axial symmetry of the hydrodynamic functions. The model course (8) of $1/\eta(z)$ as well as Δp are even in z , meanwhile the stream function A_φ , its contributions $A_{\varphi h}$ and $A_{\varphi p}$ introduced below, as well as S are odd in z . The same symmetry properties hold true for the axial Fourier transforms discussed in the next sections.

3. The Hydrodynamic Functions

3.1. Stream Function and Flow Components

We have to do with two coupled second-order partial differential equations and boundary conditions to determine the stream function $A_\varphi(r, z)$ and the vorticity function $S(r, z)$. Some peculiarities are to be observed. First, $A_\varphi(r, z)$ and $S(r, z)$ are coupled together not only through the differential equations, but also via boundary conditions. In particular, $\Delta p(r, z)$ which depends upon $A_\varphi(r, z)$ and $S(r, z)$ via (15), (17) couples back to $A_\varphi(r, z)$ through the boundary condition of the normal force balance (23). Secondly, there appear increasing z -dependent coefficients, due to the extremely increasing viscosity in axial direction. At first glance, it is not obvious whether the axial boundary condition (5) at infinite z can be satisfied at all. It is a fortunate circumstance to show that, in fact, this holds true, and in addition, the hydrodynamic functions can be represented by Fourier integrals with respect to z , so that (5) is not needed explicitly. Thirdly, to disentangle the complex problem to be solved, we will perform a refined subdivision of the hydrodynamic functions. In particular, we separate a leading part of the stream function determined through input parameters only. In what follows, an overall consistency condition is derived which must be satisfied by all other subdivided parts of the hydrodynamic functions. In this way we demonstrate, too, that the stream function and therefore, the overall viscous flux is widely governed through the balance of the normal forces at the boundaries.

Assuming, for a moment, $S(r, z)$ and $\Delta p(r, z)$ are known, the stream function $A_\varphi(r, z)$ and therefore, the overall viscous flux would be uniquely determined through the differential Equation (13) together with (17), and the boundary condition (23). That part of $A_\varphi(r, z)$ depending explicitly upon the vorticity function can be separated, subdividing $A_\varphi(r, z)$ according to

$$A_\varphi(r, z) = A_{\varphi h}(r, z) + A_{\varphi p}(r, z), \tag{25}$$

where the “homogeneous” contribution $A_{\varphi h}(r, z)$ may be solution of the homogeneous part of (13), satisfying the boundary condition (23), and vice versa, the “particular” contribution $A_{\varphi p}(r, z)$ may be solution of the inhomogeneous Equation (13), satisfying the homogeneous boundary condition

$$(\partial/\partial r)A_{\varphi p}(r, z) = 0 \text{ at } r = R_0 \text{ and } r = R_1. \tag{26}$$

Instead of $A_{\varphi h}(r, z)$, it is more convenient, at the moment, to consider the radial flux $v_{rh}(r, z)$ induced by $A_{\varphi h}(r, z)$:

$$v_{rh}(r, z) = -(\partial/\partial z)A_{\varphi h}(r, z), \tag{27}$$

which obeys

$$(\mathcal{D}_r + \partial^2/\partial z^2)v_{rh}(r, z) = 0, \tag{28}$$

to be solved with the boundary condition derived from (23)

$$\begin{aligned} & 2(\partial/\partial r)v_{rh}(r, z) \\ & = (p_0 + \Delta p(r, z)) \exp(-\alpha^2 z^2) \mp (1/r) \exp(-\alpha^2 z^2), \end{aligned} \tag{29}$$

at $r = R_0$ and $r = R_1$, with the lower sign at $r = R_1$.

According to (29), $v_{rh}(r, z)$ apparently tends to zero for $z \rightarrow \pm \infty$, which means that the radial boundary condition (29) properly implies the axial boundary condition (5). Therefore, we look for hydrodynamic functions that are ad hoc represented by Fourier integrals in z , with Fourier transforms being solutions of ad hoc Fourier-transformed differential equations and boundary conditions. Presuppositions and consistency of this treatment are in summary discussed in Appendix C.

Here and in what follows, the corresponding Fourier transforms will be denoted by a tilde. At the beginning, we will introduce

$$v_{rh}(r, z) = (1/2\pi) \int_{-\infty}^{\infty} dk \exp(ikz) \tilde{v}_{rh}(r, k). \tag{30}$$

The Fourier integral representation (30) is an important base for subsequent considerations and will be analyzed below in detail. A regular Fourier transform of $A_{\varphi h}(r, z)$ does not exist because $A_{\varphi h}(r, z)$ does not vanish (but needs not vanish) for $z \rightarrow \pm\infty$. For formal reasons and for convenience, we will introduce the *singular* Fourier transform $\tilde{A}_{\varphi h}(r, k)$ derived by a straightforward z -integration of (30) which creates a pole at $k = 0$:

$$\tilde{A}_{\varphi h}(r, k) = (i/k) \tilde{v}_{rh}(r, k). \tag{31}$$

Together with the (regular) representation of $A_{\varphi p}(r, z)$

$$A_{\varphi p}(r, z) = (1/2\pi) \int_{-\infty}^{\infty} dk \exp(ikz) \tilde{A}_{\varphi p}(r, k) \tag{32}$$

we introduce the Fourier transform $\tilde{A}_{\varphi}(r, k)$ of the total stream function according to

$$\tilde{A}_{\varphi}(r, k) = \tilde{A}_{\varphi h}(r, k) + \tilde{A}_{\varphi p}(r, k). \tag{33}$$

In addition, we provide

$$S(r, z) = (1/2\pi) \int_{-\infty}^{\infty} dk \exp(ikz) \tilde{S}(r, k). \tag{34}$$

The hydrodynamic part Δp of the pressure is needed at the boundary $r = R_0$ only, observing (22) and (23). It is convenient to introduce the ad hoc modified Fourier integral representation

$$\Delta p(R_0, z) \exp(-\alpha^2 z^2) = (1/2\pi) \int_{-\infty}^{\infty} dk \exp(ikz) \Delta \tilde{p}_1(R_0, k). \tag{35}$$

The Fourier-transformed version of (28) and (29) yields now, observing (22) and (35):

$$(\mathcal{D}_r - k^2) \tilde{v}_{rh}(r, k) = 0, \tag{36}$$

$$2(\partial/\partial r) \tilde{v}_{rh}(r, k) = (p_0 - 1/r)(\sqrt{\pi}/\alpha) \exp(-k^2/4\alpha^2) + \Delta \tilde{p}_1(R_0, k) \tag{37}$$

at $r = R_0$,

$$2(\partial/\partial r) \tilde{v}_{rh}(r, k) = (p_0 + 1/r)(\sqrt{\pi}/\alpha) \exp(-k^2/4\alpha^2) \text{ at } r = R_1. \tag{38}$$

An appropriate solution of (36) to (38) is found by series expansions in $R_1 \leq r \leq R_0$ in terms of orthonormal functions $\psi_A(n, r)$, $n = 0, 1, 2, \dots$:

$$\int_{R_1}^{R_0} dr r \psi_A(n, r) \psi_A(m, r) = \delta_{nm}, \tag{39}$$

with $\psi_A(n, r)$ being the eigenfunctions of the self-adjoint eigenvalue problem

$$\mathcal{D}_r \psi_A(n, r) = \lambda_A(n) \psi_A(n, r), \tag{40}$$

satisfying boundary conditions such as (26):

$$(d/dr) \psi_A(n, r) = 0 \text{ at } r = R_0 \text{ and } r = R_1, \tag{41}$$

δ_{nm} is the Kronecker delta, and the eigenvalues $\lambda_A(n), n = 0, 1, 2, \dots$ obey

$$0 > \lambda_A(0) > \lambda_A(1) > \dots \tag{42}$$

See Appendix A for details. Thus, we arrive at

$$\tilde{v}_{rh}(r, k) = - \sum_{n=0}^{\infty} \psi_A(n, r) \beta_A(n, k) \frac{\lambda_A(n)}{k^2 - \lambda_A(n)}, \tag{43}$$

$$\beta_A(n, k) = \beta_A^-(n) C_A^-(k, \Delta \tilde{p}_1(R_0, k)) + \beta_A^+(n) C_A^+(k, \Delta \tilde{p}_1(R_0, k), p_0), \tag{44}$$

$$C_A^-(k, \Delta \tilde{p}_1(R_0, k))$$

$$= \frac{1}{2} \left[\frac{\sqrt{\pi}}{\alpha} \exp\left(-\frac{k^2}{4\alpha^2}\right) \frac{R_0 R_1}{R_0 - R_1} - \Delta \tilde{p}_1(R_0, k) \frac{R_0^2 R_1^2}{R_0^2 - R_1^2} \right], \tag{45}$$

$$C_A^+(k, \Delta \tilde{p}_1(R_0, k), p_0)$$

$$= \frac{1}{2} \left[\frac{\sqrt{\pi}}{\alpha} \exp\left(-\frac{k^2}{4\alpha^2}\right) \left(p_0 - \frac{1}{R_0 - R_1}\right) + \Delta \tilde{p}_1(R_0, k) \frac{R_0}{R_0 - R_1} \right]. \tag{46}$$

The coefficients $\beta_A^-(n)$ and $\beta_A^+(n)$ are defined through the series expansions in $R_1 \leq r \leq R_0$

$$-1/r = \sum_{n=0}^{\infty} \psi_A(n, r) \beta_A^-(n), \text{ and } r = \sum_{n=0}^{\infty} \psi_A(n, r) \beta_A^+(n). \tag{47}$$

We continue the subdivision (25) and (33) of the total stream function, respectively, by splitting the contribution involving $\Delta \tilde{p}_1(R_0, k)$ from the (singular) Fourier transform $\tilde{A}_{\phi h}(r, k)$. Observing (45) to (47), we write

$$\tilde{A}_{\phi h}(r, k) = \tilde{A}_{\phi h}^{(0)}(r, k) + \Delta \tilde{p}_1(R_0, k) \tilde{A}_{\phi h}^{(1)}(r, k), \tag{48}$$

$$\tilde{A}_{\phi h}^{(0)}(r, k) = -\frac{\sqrt{\pi}}{\alpha} \exp\left(-\frac{k^2}{4\alpha^2}\right) \sum_{n=0}^{\infty} \psi_A(n, r) \beta_A^{(0)}(n, p_0) \frac{i}{k} \frac{\lambda_A(n)}{k^2 - \lambda_A(n)}, \tag{49}$$

$$\tilde{A}_{\phi h}^{(1)}(r, k) = - \sum_{n=0}^{\infty} \psi_A(n, r) \beta_A^{(1)}(n) \frac{i}{k} \frac{\lambda_A(n)}{k^2 - \lambda_A(n)}, \tag{50}$$

$$\beta_A^{(0)}(n, p_0) = \frac{1}{2} \cdot \left[\beta_A^-(n) \frac{R_0 R_1}{R_0 - R_1} + \beta_A^+(n) \left(p_0 - \frac{1}{R_0 - R_1}\right) \right], \tag{51}$$

$$\beta_A^{(1)}(n) = \frac{1}{2} \cdot \left[-\beta_A^-(n) \frac{R_0^2 R_1^2}{R_0^2 - R_1^2} + \beta_A^+(n) \frac{R_0^2}{R_0^2 - R_1^2} \right]. \tag{52}$$

Contrary to $A_{\phi h}(r, z)$, $A_{\phi p}(r, z)$ is represented by a regular Fourier integral (32), provided the same holds true for the same of the vorticity function (34). $\tilde{A}_{\phi p}(r, k)$ obeys the equation

$$(\mathcal{D}_r - k^2) \tilde{A}_{\phi p}(r, k) = \tilde{S}(r, k), \tag{53}$$

to be solved with the boundary condition

$$(\partial) / (\partial r) \tilde{A}_{\phi p}(r, k) = 0 \text{ at } r = R_0 \text{ and } r = R_1. \tag{54}$$

We find (see Appendix A)

$$\tilde{A}_{\phi p}(r, k) = - \sum_{n=0}^{\infty} \psi_A(n, r) \int_{R_1}^{R_0} dr_1 r_1 \psi_A(n, r_1) \frac{\tilde{S}(r_1, k)}{k^2 - \lambda_A(n)}. \tag{55}$$

The axial flow component $v_z(r, z)$ is derived from the stream function $A_\varphi(r, z)$ through the operation (12) with respect to r only. Because the Fourier transform $\tilde{A}_\varphi(r, k)$ given by (31), (33) is singular, particular attention is required to show that both $v_z(r, z)$ as well as its z -derivative are represented by regular Fourier integrals, according to

$$v_z(r, z) = (1/2\pi) \int_{-\infty}^{\infty} dk \exp(ikz) \tilde{v}_z(r, k), \tag{56}$$

$$(\partial/\partial z)v_z(r, z) = (1/2\pi) \int_{-\infty}^{\infty} dk \exp(ikz) i k \tilde{v}_z(r, k). \tag{57}$$

We will show below that (57) implies an important condition to guarantee the consistency of all hydrodynamic functions.

We will assume, for a moment, that both (56) and (57) are correct. Then (56) implies $v_z(r, z) \rightarrow 0$ for $z \rightarrow \pm \infty$, and we can further conclude, taking the inverse of the Fourier transform (57)

$$\lim_{z \rightarrow \infty} v_z(r, z) - \lim_{z \rightarrow -\infty} v_z(r, z) = \int_{-\infty}^{\infty} dz (\partial/\partial z)v_z(r, z) = \lim_{k \rightarrow 0} i k \tilde{v}_z(r, k) = 0. \tag{58}$$

The explicit representation of $\tilde{v}_z(r, k)$ is found from (12), (31), and (33) according to

$$\begin{aligned} \tilde{v}_z(r, k) = & \frac{1}{r} \frac{\partial}{\partial r} r \sum_{n=0}^{\infty} \psi_A(n, r) \frac{1}{k^2 - \lambda_A(n)} \frac{-i}{k} \left[\lambda_A(n) \beta_A(n, k) + \right. \\ & \left. + \int_{R_1}^{R_0} dr_1 r_1 \psi_A(n, r_1) \tilde{S}(r_1, k) \right]. \end{aligned} \tag{59}$$

Because $S(r, z)$ is odd in z and therefore, $\tilde{S}(r, k)$ is odd in k , we conclude $\tilde{S}(r, k) = O(k)$ for $k \rightarrow 0$, so that the second term in the bracket of (59) multiplied with the prefactor is holomorphic at $k = 0$. Thus, the condition (58) becomes

$$\lim_{k \rightarrow 0} i k \tilde{v}_z(r, k) = \frac{1}{r} \frac{\partial}{\partial r} r \sum_{n=0}^{\infty} \psi_A(n, r) \beta_A(n, 0) = 0. \tag{60}$$

$\beta_A(n, k)$ is holomorphic at $k = 0$ so that the singularity of (59) at $k = 0$ is completely removed, and both the representations (56) and (57) are regular ones.

The sum in (60) can be evaluated in closed form, applying (44) and (47) and observing $(1/r)(\partial/\partial r)r \cdot (1/r) = 0$. Summarizing, the condition (58) and (60), respectively, results in

$$\lim_{k \rightarrow 0} C_A^+(k, \Delta p_1(R_0, k), p_0) = 0. \tag{61}$$

Thus, the free pressure constant p_0 must be adjusted such that the condition (61) holds true. This requires the knowledge of $\lim_{k \rightarrow 0} \Delta p_1(R_0, k)$, which on its part requires the knowledge of a consistent set of all hydrodynamic functions including p_0 , derived below. The overall consistency is discussed in Section 3.4.

3.2. The Vorticity Function

The equation and the boundary condition of $\tilde{S}(r, k)$ are given by the Fourier-transformed version of (18) and (24), respectively. We have

$$\begin{aligned} (\mathcal{D}_r - k^2 - 4\alpha^2(\partial/\partial k)k - 2\alpha^2 + 4\alpha^4\partial^2/\partial k^2) \tilde{S}(r, k) \\ = (4\alpha^2 - 8\alpha^4\partial^2/\partial k^2) k^2 \tilde{A}_\varphi(r, k), \end{aligned} \tag{62}$$

$$\tilde{S}(r, k) = 2 \mathcal{D}_r \tilde{A}_\varphi(r, k) \quad \text{at } r = R_0 \text{ and } r = R_1. \tag{63}$$

Like (25), we subdivide $\tilde{S}(r, k)$ according to

$$\tilde{S}(r, k) = \tilde{S}_h(r, k) + \tilde{S}_p(r, k), \tag{64}$$

where $\tilde{S}_h(r, k)$ may be the solution of the homogeneous part of (62), satisfying the boundary condition (63), and vice versa, $\tilde{S}_p(r, z)$ may be the particular solution of the inhomogeneous Equation (62), satisfying the homogeneous boundary condition

$$\tilde{S}_p(r, k) = 0 \text{ at } r = R_0 \text{ and } r = R_1. \tag{65}$$

As they are Fourier transforms, $\tilde{S}_h(r, k)$ and $\tilde{S}_p(r, k)$ must satisfy, in addition,

$$\lim_{k \rightarrow \pm \infty} \tilde{S}_h(r, k) = 0. \tag{66}$$

We look for series expansions of both $\tilde{S}_h(r, k)$ and $\tilde{S}_p(r, k)$ for $R_1 \leq r \leq R_0$ in terms of orthonormal functions $\psi_Q(m, r)$, $m = 0, 1, 2, \dots$

$$\int_{R_1}^{R_0} dr r \psi_Q(n, r) \psi_Q(m, r) = \delta_{nm}, \tag{67}$$

where $\psi_Q(m, r)$ are the eigenfunctions of the self-adjoint eigenvalue problem

$$\mathcal{D}_r \psi_Q(m, r) = \lambda_Q(m) \psi_Q(m, r), \tag{68}$$

satisfying the boundary conditions

$$\psi_Q(m, r) = 0 \text{ at } r = R_0 \text{ and } r = R_1, \tag{69}$$

where the eigenvalues $\lambda_Q(m)$, $m = 0, 1, 2, \dots$ obey

$$0 > \lambda_Q(0) > \lambda_Q(1) > \dots \tag{70}$$

Equation (62) is separable and decays with

$$\tilde{S}_h(r, k) = \sum_{m=0}^{\infty} \psi_Q(m, r) \tilde{S}_{1h}(m, k), \tag{71}$$

$$\tilde{S}_p(r, k) = \sum_{m=0}^{\infty} \psi_Q(m, r) \tilde{S}_{1p}(m, k) \tag{72}$$

into a set of ordinary differential equations for $\tilde{S}_{1h}(m, k)$ and $\tilde{S}_{1p}(m, k)$, $m = 0, 1, 2, \dots$, respectively. We introduce, in addition, $\tilde{S}_{2h}(m, k)$ and $\tilde{S}_{2p}(m, k)$ by means of the substitution

$$\tilde{S}_{1h}(m, k) = \exp(k^2/4\alpha^2) \tilde{S}_{2h}(m, k), \tag{73}$$

$$\tilde{S}_{1p}(m, k) = \exp(k^2/4\alpha^2) \tilde{S}_{2p}(m, k). \tag{74}$$

$\tilde{S}_{2h}(m, k)$ and $\tilde{S}_{2p}(m, k)$ obey differential equations with identical differential operator and boundary conditions, but with different inhomogeneous terms. Meanwhile the derivation for $\tilde{S}_{2p}(m, k)$ is straightforward, more effort is required with respect to $\tilde{S}_{2h}(m, k)$ (see Appendix B). We find

$$\mathcal{L}(m) \tilde{S}_{2p}(m, k) = \tilde{F}_h(m, k) + \tilde{F}_p(m, k), \tag{75}$$

$$\mathcal{L}(m) \tilde{S}_{2h}(m, k) = \tilde{F}_{2h}(m, k), \tag{76}$$

$$\lim_{k \rightarrow \pm \infty} \tilde{S}_{2p}(m, k) = 0 \text{ and } \lim_{k \rightarrow \pm \infty} \tilde{S}_{2h}(m, k) = 0, \tag{77}$$

where $\mathcal{L}(m)$ abbreviates the differential operator

$$\mathcal{L}(m) \equiv d^2/dk^2 + \lambda_Q(m)/4\alpha^2 - 1/\alpha^2 - (1/2\alpha^4)k^2. \tag{78}$$

Thus, we can summarize

$$\tilde{S}_2(m, k) = \tilde{S}_{2p}(m, k) + \tilde{S}_{2h}(m, k), \tag{79}$$

$$\mathcal{L}(m) \tilde{S}_2(m, k) = \tilde{F}_2(m, k), \tag{80}$$

$$\lim_{k \rightarrow \pm\infty} \tilde{S}_2(m, k) = 0, \tag{81}$$

$$\tilde{F}_2(m, k) = \tilde{F}_h(m, k) + \tilde{F}_p(m, k) + \tilde{F}_{2h}(m, k), \tag{82}$$

where the expressions on the r. h. s. of (82) are

$$\tilde{F}_p(m, k) = \int_{R_1}^{R_0} dr r \psi_Q(m, r) \exp\left(-\frac{k^2}{4\alpha^2}\right) \left(\frac{1}{\alpha^2} - 2\frac{\partial^2}{\partial k^2}\right) k^2 \tilde{A}_{\varphi_p^h}(r, k), \tag{83}$$

$$\begin{aligned} \tilde{F}_{2h}(m, k) &= (\lambda_Q(m)/4\alpha^4) \times \\ &\times (\beta_Q^-(m) C_S^{(-)}(k, \Delta p_1(R_0, k), p_0) + \beta_Q^+(m) C_S^{(+)}(k, \Delta p_1(R_0, k), p_0)), \end{aligned} \tag{84}$$

$$\begin{aligned} &C_S^{(-)}(k, \Delta p_1(R_0, k), p_0) \\ &= -\frac{R_0 R_1}{R_0^2 - R_1^2} \left(R_0 \Phi(R_1, k, \Delta p_1(R_0, k), p_0) - R_1 \Phi(R_0, k, \Delta p_1(R_0, k), p_0) \right), \end{aligned} \tag{85}$$

$$\begin{aligned} &C_S^{(+)}(k, \Delta p_1(R_0, k), p_0) \\ &= \frac{1}{R_0^2 - R_1^2} \left(R_0 \Phi(R_0, k, \Delta p_1(R_0, k), p_0) - R_1 \Phi(R_1, k, \Delta p_1(R_0, k), p_0) \right), \end{aligned} \tag{86}$$

$$\begin{aligned} &\Phi(r, k, \Delta p_1(R_0, k), p_0) \\ &= -2 \exp\left(-\frac{k^2}{4\alpha^2}\right) k^2 \left[\tilde{A}_{\varphi^h}^{(0)}(r, k) + \Delta \tilde{p}_1(R_0, k) \tilde{A}_{\varphi^h}^{(1)}(r, k) + \tilde{A}_{\varphi^p}(r, k) \right]. \end{aligned} \tag{87}$$

The dependence of $\Phi(r, k, \Delta p_1(R_0, k), p_0)$ upon p_0 arises from $\tilde{A}_{\varphi^h}^{(0)}(r, k)$ through (49) and (51).

The coefficients $\beta_Q^-(m), \beta_Q^+(m)$ are defined through the series expansions in $R_1 \leq r \leq R_0$ according to

$$-1/r = \sum_{m=0}^{\infty} \psi_Q(m, r) \beta_Q^-(m), \text{ and } r = \sum_{m=0}^{\infty} \psi_Q(m, r) \beta_Q^+(m). \tag{88}$$

We note that the singularity of $\tilde{A}_{\varphi^h}(r, k)$ at $k = 0$ is removed on the r. h. s. of (82). Details of the derivation are given in Appendix B.

If both the r. h. s. of (62) and (63) are square-integrable in $-\infty \leq k \leq \infty$, $\tilde{F}_2(m, k)$ given by (82) is square-integrable in $-\infty \leq k \leq \infty$, too. This is the precondition to determine $\tilde{S}_2(m, k), m = 0, 1, 2, \dots$ through solution of (79) to (81) based on a regular eigenvalue problem defined for the infinite k -interval $-\infty \leq k \leq \infty$. In particular, we get the series expansions in terms of the orthonormal functions $\psi_{S_2}(p, k), p = 0, 1, 2, \dots$ in $-\infty \leq k \leq \infty$, according to

$$\tilde{S}_2(m, k) = \sum_{p=0}^{\infty} s_2(m, p) \psi_{S_2}(p, k), \tag{89}$$

$$\int_{-\infty}^{\infty} dk \psi_{S_2}(p, k) \psi_{S_2}(q, k) = \delta_{pq}, \tag{90}$$

where $\psi_{S2}(p, k)$ are the eigenfunctions of the regular self-adjoint eigenvalue problem

$$\mathcal{L}(m) \psi_{S2}(p, k) = \lambda_{S2}(m, p) \psi_{S2}(p, k), \tag{91}$$

$$\lim_{k \rightarrow \pm\infty} \psi_{S2}(p, k) = 0. \tag{92}$$

$\psi_{S2}(p, k)$ and $\lambda_{S2}(m, p)$ are given by

$$\psi_{S2}(p, k) = (1/\sqrt{2^{1/4}\alpha}) \psi(p, k/2^{1/4}\alpha), \tag{93}$$

and

$$\lambda_{S2}(m, p) = -(1/\sqrt{2}\alpha^2) (1 + \sqrt{2} + 2p) + (1/4\alpha^4)\lambda_Q(m), \tag{94}$$

respectively, where

$$\psi(n, x) = (2^n n! \sqrt{\pi})^{-1/2} \exp(-x^2/2)H(n, x) \tag{95}$$

is the ‘‘physical’’ Hermite function (see, e.g., [33]), and $H(n, x)$ is the Hermite polynomial of the order n . Because the inhomogeneous term $\tilde{F}_2(m, k)$ given by (82) can be expanded as

$$\tilde{F}_2(m, k) = \sum_{p=0}^{\infty} f_2(m, p) \psi_{S2}(p, k), \tag{96}$$

the coefficients $s_2(m, p)$ of (89) are given by

$$s_2(m, p) = f_2(m, p) / \lambda_{S2}(m, p). \tag{97}$$

For symmetry reasons, we must have $s_2(m, p) = 0$ for even p . The eigenvalues $\lambda_{S2}(m, p)$, $p = 0, 1, 2, \dots$ form an equidistant sequence without finite limiting value.

The Fourier transform of the vorticity function $\tilde{S}(r, k)$ follows through combining (89), (71) to (74) and (64). We arrive at the convergent series expansion

$$\tilde{S}(r, k) = \sum_{m=0}^{\infty} \psi_Q(m, r) \sum_{p=0}^{\infty} s_2(m, p) \psi_{S2}(p, k) \exp(k^2/4\alpha^2). \tag{98}$$

We note that $\psi_{S2}(p, k) \exp(k^2/4\alpha^2) \propto k^p \exp(-(\sqrt{2} - 1)k^2/4\alpha^2) \rightarrow 0$ for $k \rightarrow \pm\infty$. In practice, $\tilde{S}(r, k)$ will be approached by $\tilde{S}_{m_1, p_1}(r, k)$ where the sum (98) is truncated at $m = m_1$ and $p = p_1$. Therefore $\tilde{S}_{m_1, p_1}(r, k)$ obeys

$$\tilde{S}_{m_1, p_1}(r, k) \propto k^{p_1} \exp(-(\sqrt{2} - 1)k^2/4\alpha^2) \rightarrow 0 \text{ for } k \rightarrow \pm\infty, \tag{99}$$

which is the precondition of $\tilde{S}_{m_1, p_1}(r, k)$ being a Fourier transform, too. Because of the convergence of (98), we have

$$\tilde{S}(r, k) = \lim_{m_1 \rightarrow \infty} \lim_{p_1 \rightarrow \infty} \tilde{S}_{m_1, p_1}(r, k). \tag{100}$$

The sum (98) and the limiting process (100), respectively, converge rather poorly. As shown below, we need $\tilde{S}(r, k)$ in the limit $k \rightarrow 0$ to calculate collapsing-relevant parameters. Because the accuracy of this limiting value depends upon the truncation indices, this is a typical situation to succeed in an analytical work applying computer-aided tools.

3.3. The Pressure

We rewrite (15). Regarding (8), (17), and (21), we find:

$$\exp(-\alpha^2 z^2) \frac{\partial}{\partial r} \Delta p(r, z) = -\left(\frac{\partial}{\partial z} + 2\alpha^2 z\right) S(r, z) + 4\alpha^2 z \mathcal{D}_r A_\varphi(r, z). \tag{101}$$

Observing (22) and (35), the Fourier transform of $\Delta p(R_0, z) \exp(-\alpha^2 z^2)$ obeys

$$\begin{aligned} \Delta \tilde{p}_1(R_0, k) = & -i \int_{R_1}^{R_0} dr (k + 2\alpha^2 \frac{\partial}{\partial k}) \tilde{S}(r, k) + 4\alpha^2 i \int_{R_1}^{R_0} dr \frac{\partial}{\partial k} \mathcal{D}_r \tilde{A}_{\phi p}(r, k) \\ & + 4\alpha^2 i \int_{R_1}^{R_0} dr \frac{\partial}{\partial k} \mathcal{D}_r \tilde{A}_{\phi h}(r, k). \end{aligned} \tag{102}$$

(102) shows that $\Delta \tilde{p}_1(R_0, k)$ consists of two parts depending upon the stream function and vorticity function only, respectively. According to (48), $\tilde{A}_{\phi h}(r, k)$ consists of two parts, too, where $\tilde{A}_{\phi h}^{(0)}(r, k)$ directly depends upon the experimental input parameters, meanwhile the residual explicitly depends upon $\Delta \tilde{p}_1(R_0, k)$. We rearrange (102) to collect all terms involving $\Delta \tilde{p}_1(R_0, k)$ on the l. h. s. We arrive at

$$\begin{aligned} \Delta \tilde{p}_1(R_0, k) - 4\alpha^2 i \Delta \tilde{p}_1(R_0, k) \int_{R_1}^{R_0} dr \frac{\partial}{\partial k} \mathcal{D}_r \tilde{A}_{\phi h}^{(1)}(r, k) \\ - 4\alpha^2 i \left[\frac{\partial}{\partial k} \Delta \tilde{p}_1(R_0, k) \right] \int_{R_1}^{R_0} dr \mathcal{D}_r \tilde{A}_{\phi h}^{(1)}(r, k) \\ = 4\alpha^2 i \int_{R_1}^{R_0} dr \frac{\partial}{\partial k} \mathcal{D}_r \tilde{A}_{\phi h}^{(0)}(r, k) \\ - i \int_{R_1}^{R_0} dr (k + 2\alpha^2 \frac{\partial}{\partial k}) \tilde{S}(r, k) + 4\alpha^2 i \int_{R_1}^{R_0} dr \frac{\partial}{\partial k} \mathcal{D}_r \tilde{A}_{\phi p}(r, k). \end{aligned} \tag{103}$$

Thus, the apparently straightforward relation (101) turns out to become the linear, inhomogeneous, first-order differential Equation (103) for $\Delta \tilde{p}_1(R_0, k)$, where the solution must satisfy

$$\lim_{k \rightarrow \pm\infty} \Delta \tilde{p}_1(R_0, k) = 0. \tag{104}$$

Obviously, $\Delta \tilde{p}_1(R_0, k)$ can be split in two parts

$$\Delta \tilde{p}_1(R_0, k) = \Delta \tilde{p}_{1A}(R_0, k) + \Delta \tilde{p}_{1S}(R_0, k), \tag{105}$$

and (103) decays into two equations

$$\Delta \tilde{p}_{1A}(R_0, k) + \mathcal{P}_1 \{ \Delta \tilde{p}_{1A} \} = P_A(k), \tag{106}$$

$$\Delta \tilde{p}_{1S}(R_0, k) + \mathcal{P}_1 \{ \Delta \tilde{p}_{1S} \} = \mathcal{P}_S \{ \tilde{S} \}. \tag{107}$$

For evaluation, we apply $\mathcal{D}_r A_{\phi h}(r, k) = k^2 A_{\phi h}(r, k)$. Then the operators \mathcal{P}_1 and \mathcal{P}_S abbreviate

$$\mathcal{P}_1 \{ \tilde{f} \} = -4\alpha^2 i \int_{R_1}^{R_0} dr \frac{\partial}{\partial k} \left[\tilde{f}(k) \sum_{n=0}^{\infty} \psi_A(n, r) \beta_A^{(1)}(n) \frac{-ik\lambda_A(n)}{k^2 - \lambda_A(n)} \right], \tag{108}$$

$$\begin{aligned} \mathcal{P}_S \{ \tilde{S} \} = & -i \int_{R_1}^{R_0} dr (k + 2\alpha^2 \frac{\partial}{\partial k}) \tilde{S}(r, k) + 4\alpha^2 i \int_{R_1}^{R_0} dr \frac{\partial}{\partial k} \mathcal{D}_r \tilde{A}_{\phi p}(r, k) \\ = & -i \int_{R_1}^{R_0} dr (k + 2\alpha^2 \partial / \partial k) \tilde{S}(r, k) \\ & - 4\alpha^2 i \int_{R_1}^{R_0} dr \frac{\partial}{\partial k} \left[\sum_{n=0}^{\infty} \int_{R_1}^{R_0} dr_1 \psi_A(n, r) r_1 \psi_A(n, r_1) \frac{\lambda_A(n) \tilde{S}(r_1, k)}{k^2 - \lambda_A(n)} \right], \end{aligned} \tag{109}$$

respectively, and $P_A(k)$ denotes

$$P_A(k) = 4\alpha^2 i \int_{R_1}^{R_0} dr \frac{\partial}{\partial k} \left[\frac{\sqrt{\pi}}{\alpha} \exp\left(-\frac{k^2}{4\alpha^2}\right) \sum_{n=0}^{\infty} \psi_A(n, r) \beta_A^{(0)}(n, p_0) \frac{-ik\lambda_A(n)}{k^2 - \lambda_A(n)} \right]. \tag{110}$$

Solutions of (106), (107) must be found which satisfy, analogously to (104),

$$\lim_{k \rightarrow \pm\infty} \Delta \tilde{p}_{1A}(R_0, k) = 0 \quad \text{and} \quad \lim_{k \rightarrow \pm\infty} \Delta \tilde{p}_{1S}(R_0, k) = 0. \tag{111}$$

$\Delta \tilde{p}_{1A}(R_0, k)$ corresponds to that part of the variable pressure which is directly induced through the experimental input parameters, meanwhile $\Delta \tilde{p}_{1S}(R_0, k)$ is attributed to the indirect contribution via $\tilde{A}_{\varphi p}(r, k)$ and $\tilde{S}(r, k)$.

The solution of the differential Equations (106) and (107) satisfying (111) is a non-trivial task. As shown in Appendix C, the infinite sums involved in (108) and (110) are meromorphic functions of k with singularities on the imaginary k -axis only, and there exists a strip $\mathcal{K} := \{ | \Im k | < a \}$, $0 < a \leq \sqrt{|\lambda_A(0)|}$ along the real k -axis where the coefficients of the differential Equations (106) and (107) are holomorphic. We must look for particular solutions that are holomorphic for $k \in \mathcal{K}$ and vanish for $k \in \mathcal{K}$, $k \rightarrow \pm\infty$. Our approach is predetermined by the basic theorem on local, regular, analytic solutions of differential equations and their analytic continuation [34].

We start with (106), which may be abbreviated as

$$\Delta \tilde{p}_{1A}(R_0, k) = (d/dk) \left(g_0(k) \cdot \Delta \tilde{p}_{1A}(R_0, k) + g_1(k) \cdot \exp(-k^2/4\alpha^2) \right). \tag{112}$$

$g_0(k)$ and $g_1(k)$ are odd functions, holomorphic for $k \in \mathcal{K}$, and $O(k)$ for $k \rightarrow 0$. Then it is verified by a power series ansatz at $k = 0$ that a unique and even solution $\Delta \tilde{p}_{1A}(R_0, k)$ which is $O(1)$ for $k \rightarrow 0$ only exists if $g_1(k) \not\equiv 0$, i.e., for the particular solution of (112) exclusively. These power series converge for $|k| < \sqrt{-\lambda_A(0)}$ only, but can be analytically continued to be a holomorphic function for all $k \in \mathcal{K}$. To succeed for $k \rightarrow \pm\infty$, we note that $g_0(k) = O(1)$, $g_1(k) = O(1)$ for $k \in \mathcal{K}$, $k \rightarrow \pm\infty$ (see Appendix C). Then the comparison of the leading order of (112) for $k \rightarrow \pm\infty$ yields the asymptotic behavior

$$\Delta \tilde{p}_{1A}(R_0, k) = \exp(-k^2/4\alpha^2) \cdot O(1) \quad \text{for} \quad k \rightarrow \pm\infty. \tag{113}$$

Based the presupposition of $\tilde{S}(r, k)$ outlined and verified in Appendix C, a similar analysis can be carried out for (107) to show that $\Delta \tilde{p}_{1S}(R_0, k)$ is holomorphic for $k \in \mathcal{K}$, with the asymptotic behavior (A43). We refer to Appendix C.

To represent the solution of (106) for the entire k -range it is suggested to determine $\Delta \tilde{p}_{1A}(R_0, k)$ as series expansion for $-\infty \leq k \leq \infty$ in terms of orthonormal, adjusted Hermitian functions

$$\psi_{PA}(p, k) = (1/\sqrt{2^{1/2}\alpha}) \psi(p, k/2^{1/2}\alpha), \quad p = 0, 2, 4, \dots \tag{114}$$

which involve the exponential $\exp(-k^2/4\alpha^2)$, like $P_A(k)$ in (106). Our starting ansatz is the truncated series expansion

$$\Delta \tilde{p}_{1A}(R_0, k) = \sum_{q=0}^{p_2} b_A(q) \psi_{PA}(q, k). \tag{115}$$

We substitute (115) on the l. h. s. of (106) and introduce the truncated series expansions on both the l. h. s. and r. h. s. of (106) in terms of $\psi_{PA}(q, k)$, according to

$$P_A(k) = \sum_{q=0}^{p_2} b_{PA}(q) \psi_{PA}(q, k), \tag{116}$$

$$\mathcal{P}_1 \{ \psi_{PA}(q, k) \} = \sum_{q_1=q}^{p_2} \Lambda_{P1}(q, q_1) \psi_{PA}(q_1, k), \tag{117}$$

where $b_A(q) = 0, b_{PA}(q) = 0$ for odd $q, \Lambda_{P1}(q, q_1) = 0$ for odd $q - q_1$. Through comparison of coefficients, we get the linear equation system

$$b_A(q) + \sum_{q_1=0}^{p_2} \Lambda_{P1}(q_1, q) b_A(q_1) = b_{PA}(q), \quad q = 0, 2, \dots, p_2 \text{ even}, \tag{118}$$

to determine $b_A(q), q = 0, 2, \dots, p_2$ even, which enter (115).

To determine $\Delta\tilde{p}_{1S}(R_0, k)$ as solution of (107), we first substitute $\tilde{S}(r, k)$ given by (98) into (107), noting that the coefficients $s_2(m, p)$ are yet unknown. Because (107) is linear, $\Delta\tilde{p}_{1S}(R_0, k)$ is given as superposition of elementary contributions $\Delta\tilde{q}_S(m, p; k)$ for all indices $\{m, p\}$. The starting ansatz is the truncated series

$$\Delta\tilde{p}_{1S}(R_0, k) = \sum_{m=0}^{m_2} \sum_{p=0}^{p_1} s_2(m, p) \Delta\tilde{q}_S(m, p; k), \tag{119}$$

where $\Delta\tilde{q}_S(m, p; k)$ is solution of

$$\begin{aligned} \Delta\tilde{q}_S(m, p; k) + \mathcal{P}_1 \{ \Delta\tilde{q}_S(m, p; k) \} &= \mathcal{P}_S \{ \psi_Q(m, r) \psi_{S2}(p, k) \exp(k^2/4\alpha^2) \}, \\ m = 0, 1, 2, \dots, m_1, \quad p = 1, 3, \dots, p_1, \quad p_1 \text{ odd}, \\ \Delta\tilde{q}_S(m, p; k) &= 0, \quad p \text{ even}. \end{aligned} \tag{120}$$

(120) can be solved analogously to (106). The r. h. s. of (120) involves the exponential $\exp(-(\sqrt{2}-1)k^2/4\alpha^2)$, as concluded from (99), (109). Therefore, it is suggested to look for $\Delta\tilde{q}_S(m, p; k)$ as series expansion for $-\infty \leq k \leq \infty$ in terms of the orthonormal, adjusted Hermitian functions $\psi_{PS}(p, k)$ given by

$$\psi_{PS}(p, k) = ((\sqrt{2}-1)/2)^{1/4} \alpha^{-1/2} \psi(p, ((\sqrt{2}-1)/2)^{1/2} k/\alpha). \tag{121}$$

We choose

$$\Delta\tilde{q}_S(m, p; k) = \sum_{q=0}^{p_1} b_S(m, p, q) \psi_{PS}(q, k), \tag{122}$$

where $b_S(m, p, q) = 0$ for even q , and introduce the truncated series expansions

$$\mathcal{P}_S \{ \psi_Q(m, r) \psi_{S2}(p, k) \} = \sum_{q=0}^{p_1} b_{PS}(m, p, q) \psi_{PS}(q, k), \tag{123}$$

$$\mathcal{P}_1 \{ \psi_{S2}(q, k) \} = \sum_{q_1=0}^{p_1} \Lambda_{S1}(q, q_1) \psi_{PS}(q_1, k), \tag{124}$$

where $b_{PS}(m, p, q) = 0$ for even p and q , and $\Lambda_{S1}(q, q_1) = 0$ for odd $q - q_1$. If substituted into (120), the coefficients $b_S(m, p, q)$ which enter (122) are determined by comparison of coefficients through the linear equation system

$$\begin{aligned} b_S(m, p, q) + \sum_{q_1=0}^{p_1} \Lambda_{S1}(q_1, q) b_S(m, p, q_1) &= b_{PS}(m, p, q) \\ p = 1, 3, \dots, p_1, \quad q = 1, 3, \dots, p_1, \quad p_1 \text{ odd}. \end{aligned} \tag{125}$$

We note that the coefficients $b_A(q)$ and $b_S(m, p, q)$ also depend upon the truncation indices p_2 , and p_1 , respectively.

Finally, we show that $\Delta\tilde{p}_1(R_0, k)$ given by the starting relation (102) can be evaluated in almost closed form in the limit $k \rightarrow 0$. First, we rewrite the last term on the r. h. s. of (102), observing (31) and (43):

$$4\alpha^2 i \int_{R_1}^{R_0} dr \frac{\partial}{\partial k} \mathcal{D}_r \tilde{A}_{\phi h}(r, k) = 4\alpha^2 i \int_{R_1}^{R_0} dr \frac{\partial}{\partial k} \mathcal{D}_r \sum_{n=0}^{\infty} \psi_A(n, r) \beta_A(n, k) \frac{i}{k} \left[-1 + \frac{k^2}{k^2 - \lambda_A(n)} \right]. \tag{126}$$

Substituting $\beta_A(n, k)$ by (44), the sum on the r. h. s. of (126) can be evaluated with respect to the first term of the bracket, observing (47), which yields zero because of $\mathcal{D}_r(1/r) = 0$ and $\mathcal{D}_r r = 0$. With respect to the second term of the bracket, we apply (40) and use that $\beta_A(n, k)$ is even in k , holomorphic and non-vanishing around $k = 0$. Then the series expansion at $k = 0$ yields

$$4\alpha^2 i \int_{R_1}^{R_0} dr \frac{\partial}{\partial k} \mathcal{D}_r \tilde{A}_{\phi h}(r, k) = 4\alpha^2 \int_{R_1}^{R_0} dr \sum_{n=0}^{\infty} \psi_A(n, r) (\beta_A(n, 0) + O(k^2)). \tag{127}$$

Again, the sum on the r. h. s. of (127) can be evaluated observing (47), and $\beta_A(n, 0)$ can be substituted by (44), where, in addition, (61) must be observed. We arrive at

$$\begin{aligned} \lim_{k \rightarrow 0} 4\alpha^2 i \int_{R_1}^{R_0} dr \frac{\partial}{\partial k} \mathcal{D}_r \tilde{A}_{\phi h}(r, k) &= 4\alpha^2 \log\left(\frac{R_0}{R_1}\right) C_A^-(0, \Delta\tilde{p}_1(R_0, 0)) \\ &= 2\alpha^2 \log\left(\frac{R_0}{R_1}\right) \left[\frac{\sqrt{\pi}}{\alpha} \frac{R_0 R_1}{R_0 - R_1} - \Delta\tilde{p}_1(R_0, 0) \frac{R_0^2 R_1^2}{R_0^2 - R_1^2} \right], \end{aligned} \tag{128}$$

The remaining contribution on the r. h. s. of (103) equals $\mathcal{P}_S\{\tilde{S}\}$ given by (109). With respect to the last term on the r. h. s. of (109), we first carry out the Taylor expansion at $k = 0$ and find

$$\sum_{n=0}^{\infty} \int_{R_1}^{R_0} dr_1 \psi_A(n, r) r_1 \psi_A(n, r_1) \frac{\lambda_A(n) \tilde{S}(r_1, k)}{k^2 - \lambda_A(n)} = -k \left[(\partial/\partial k) \tilde{S}(r, k) \right]_{k=0} + O(k^3). \tag{129}$$

It is taken into account here that $\tilde{S}(r, k)$ is odd in k , and that the Dirac δ -function appears in the order k^1 of the Taylor expansion so that the sum of n can be evaluated again. The overall result is

$$\lim_{k \rightarrow 0} \mathcal{P}_S\{\tilde{S}\} = 2\alpha^2 i \lim_{k \rightarrow 0} \int_{R_1}^{R_0} dr (\partial/\partial k) \tilde{S}(r, k). \tag{130}$$

Observing (128), (103) taken in the limit $k \rightarrow 0$ becomes a linear algebraic equation for $\Delta\tilde{p}_1(R_0, 0)$. The solution is

$$\begin{aligned} &\Delta\tilde{p}_1(R_0, 0) \\ &= 2\alpha^2 \frac{(\sqrt{\pi}/\alpha) \log(R_0/R_1) \cdot R_0 R_1 / (R_0 - R_1) + i \lim_{k \rightarrow 0} \int_{R_1}^{R_0} dr (\partial/\partial k) \tilde{S}(r, k)}{1 + 2\alpha^2 \log(R_0/R_1) \cdot R_0^2 R_1^2 / (R_0^2 - R_1^2)}. \end{aligned} \tag{131}$$

The dependence of $\Delta\tilde{p}_1(R_0, 0)$ upon the vorticity function is available as series expansion only. We find from $\tilde{S}(r, k)$ given by (98):

$$\begin{aligned} &\lim_{k \rightarrow 0} \int_{R_1}^{R_0} dr (\partial/\partial k) \tilde{S}(r, k) \\ &= \lim_{k \rightarrow 0} \sum_{m=0}^{\infty} \int_{R_1}^{R_0} dr \psi_Q(m, r) \sum_{p=0}^{\infty} (\partial/\partial k) s_2(m, p) \psi_{S_2}(p, k) \exp(k^2/4\alpha^2) \end{aligned}$$

$$= \sum_{m=0}^{\infty} \int_{R_1}^{R_0} dr \psi_Q(m, r) \sum_{p=0}^{\infty} s_2(m, p) \frac{\pi^{1/4} p^{2p/2}}{2^{3/8} \alpha^{3/2} \sqrt{p!} \Gamma(\frac{2-p}{2})}, \tag{132}$$

with Γ as the Euler gamma function.

3.4. Rearrangement and Consistency

The subdivision (105) of $\Delta \tilde{p}_1(R_0, k)$ is the guide to rearrange the stream function as a whole. We start with

$$\tilde{A}_\varphi(r, k) = \tilde{A}_\varphi^{(A)}(r, k) + \tilde{A}_\varphi^{(S)}(r, k). \tag{133}$$

$\tilde{A}_\varphi^{(A)}(r, k)$ is that part separated from the stream function, which depends upon experimental input parameters only, i.e., without feedback from other contributions. Because $\tilde{A}_\varphi(r, k)$ is governed through the normal forces balance at the boundaries, $\tilde{A}_\varphi^{(A)}(r, k)$ must include $\Delta \tilde{p}_{1A}(R_0, k)$ being solution of (106) and given by (115). $\tilde{A}_\varphi^{(A)}(r, k)$ also depends upon p_0 via $\tilde{A}_{\varphi h}^{(0)}(r, k)$. For clarity, we will widely omit p_0 in this subsection and take up it at the end. We have therefore

$$\tilde{A}_\varphi^{(A)}(r, k) = \tilde{A}_{\varphi h}^{(0)}(r, k) + \Delta \tilde{p}_{1A}(R_0, k) \tilde{A}_{\varphi h}^{(1)}(r, k). \tag{134}$$

$\tilde{A}_\varphi^{(S)}(r, k)$ collects the remaining parts of the stream function, where all of them depend upon $\tilde{S}(r, k)$. Observing (25), (48), (105), and (55), we have

$$\tilde{A}_\varphi^{(S)}(r, k) = \Delta \tilde{p}_{1S}(R_0, k) \tilde{A}_{\varphi h}^{(1)}(r, k) + \tilde{A}_{\varphi p}(r, k). \tag{135}$$

Starting from known input parameters, the vorticity function is the yet missing contribution to calculate the whole stream function $A_\varphi(r, z)$ and the viscous flow. This is the matter of the outstanding overall consistency condition. In what follows, the latter will be derived in three steps.

First, other occurring functions, if represented as linear expressions in $\tilde{A}_\varphi(r, k)$, will be rearranged like (133). We will use the superscript (A) and (S), too, to indicate the dependence upon $\tilde{A}_\varphi^{(A)}(r, k)$ and $\tilde{A}_\varphi^{(S)}(r, k)$ only, respectively, noting that (A) also indicates the explicit dependence upon p_0 .

Starting with (87), the substitution of (133) to (135) on the r. h. s. yields

$$\Phi(r, k, \Delta p_1(R_0, k), p_0) = \Phi^{(A)}(r, k) + \Phi^{(S)}(r, k), \tag{136}$$

$$\Phi^{(A)}(r, k) = -2 \exp\left(-\frac{k^2}{4\alpha^2}\right) k^2 \tilde{A}_\varphi^{(A)}(r, k), \tag{137}$$

$$\Phi^{(S)}(r, k) = -2 \exp\left(-\frac{k^2}{4\alpha^2}\right) k^2 \tilde{A}_\varphi^{(S)}(r, k). \tag{138}$$

The subdivision (136) can be traced back from (87) to (84), leading to a likewise rearrangement according to

$$\tilde{F}_{2h}(m, k) = \tilde{F}_{2h}^{(A)}(m, k) + \tilde{F}_{2h}^{(S)}(m, k). \tag{139}$$

In the same way, (82) can be rearranged, starting from (83)

$$\tilde{F}_h(m, k) + \tilde{F}_p(m, k) = \tilde{F}_{hp}^{(A)}(m, k) + \tilde{F}_{hp}^{(S)}(m, k), \tag{140}$$

$$\begin{aligned} & \tilde{F}_{hp}^{(A)}(m, k) \\ &= \int_{R_1}^{R_0} dr r \psi_Q(m, r) \exp\left(-\frac{k^2}{4\alpha^2}\right) \left(\frac{1}{\alpha^2} - 2\frac{\partial^2}{\partial k^2}\right) k^2 \tilde{A}_\varphi^{(A)}(r, k), \end{aligned} \tag{141}$$

$$\begin{aligned} & \tilde{F}_{hp}^{(S)}(m, k) \\ = & \int_{R_1}^{R_0} dr r \psi_Q(m, r) \exp\left(-\frac{k^2}{4\alpha^2}\right) \left(\frac{1}{\alpha^2} - 2\frac{\partial^2}{\partial k^2}\right) k^2 \tilde{A}_\varphi^{(S)}(r, k), \end{aligned} \tag{142}$$

so that we arrive at

$$\tilde{F}_2(m, k) = \tilde{F}_2^{(A)}(m, k) + \tilde{F}_2^{(S)}(m, k), \tag{143}$$

$$\tilde{F}_2^{(A)}(m, k) = \tilde{F}_{hp}^{(A)}(m, k) + \tilde{F}_{2h}^{(A)}(m, k), \tag{144}$$

$$\tilde{F}_2^{(S)}(m, k) = \tilde{F}_{hp}^{(S)}(m, k) + \tilde{F}_{2h}^{(S)}(m, k). \tag{145}$$

Secondly, we show that even the vorticity function can be formally rearranged, following the schema (133). Substituting (143) on the r. h. s. of (80), the set of linear, inhomogeneous differential Equations (80) becomes split according to

$$\tilde{S}_2(m, k) = \tilde{S}_2^{(A)}(m, k) + \tilde{S}_2^{(S)}(m, k), \tag{146}$$

$$\mathcal{L}(m) \tilde{S}_2^{(A)}(m, k) = \tilde{F}_2^{(A)}(m, k), \tag{147}$$

$$\mathcal{L}(m) \tilde{S}_2^{(S)}(m, k) = \tilde{F}_2^{(S)}(m, k), \tag{148}$$

$m = 0, 1, 2, \dots$, to be solved with the boundary conditions

$$\lim_{k \rightarrow \pm\infty} \tilde{S}_2^{(S)}(m, k) = 0. \tag{149}$$

$\tilde{S}_2^{(A)}(m, k)$ and $\tilde{S}_2^{(S)}(m, k)$ are solutions of the mutually independent differential Equations (147) and (148), respectively, where $\tilde{S}_2^{(A)}(m, k)$ is determined through $\tilde{A}_\varphi^{(A)}(r, k)$ only, i.e., through the experimental input parameters only, and $\tilde{S}_2^{(S)}(m, k)$ is determined through $\tilde{A}_\varphi^{(S)}(r, k)$, i.e., through the (Fourier-transformed) vorticity function $\tilde{S}(r, k)$ itself. Thus, (146) is the key to determine the vorticity function self-consistently.

(147) together with (149) can be solved, strictly following the outlined schema (89) to (97) how to solve (80), (81). The adequate ansatzes are

$$\tilde{F}_2^{(A)}(m, k) = \sum_{p=0}^{\infty} f_2^{(A)}(m, p) \psi_{s2}(p, k), \tag{150}$$

$$\tilde{S}_2^{(A)}(m, k) = \sum_{p=0}^{\infty} s_2^{(A)}(m, p) \psi_{s2}(p, k), \tag{151}$$

$$s_2^{(A)}(m, p) = f_2^{(A)}(m, p) / \lambda_{s2}(m, p). \tag{152}$$

Thirdly, we determine $\tilde{S}_2^{(S)}(m, k)$ by formal solution of (148), (149). It is provided that $\tilde{S}(r, k)$ involved in $\tilde{F}_2^{(S)}(m, k)$ is represented by the series (98). Then $\tilde{F}_2^{(S)}(m, k)$ given by (145) can be decomposed as series according to (98). The key is the linear dependence of $\tilde{F}_2^{(S)}(m, k)$ upon $\tilde{A}_\varphi^{(S)}(r, k)$ where, vice versa, $\tilde{A}_\varphi^{(S)}(r, k)$ given by (135) is a linear expression in $\tilde{S}(r, k)$. We therefore start with $\tilde{A}_\varphi^{(S)}(r, k)$, which will be ad hoc represented as series in terms of superposed elementary contributions $\tilde{A}_\varphi^{(SE)}(m, p, r, k)$ with coefficients $s_2(m, p)$ according to

$$\tilde{A}_\varphi^{(S)}(r, k) = \sum_{m=0}^{\infty} \sum_{p=0}^{p_1} s_2(m, p) \tilde{A}_\varphi^{(SE)}(m, p; r, k), \tag{153}$$

where $\tilde{A}_\varphi^{(SE)}(m, p; r, k) = 0$ for even p . Thus, the decomposition of (135) results is

$$\begin{aligned} \tilde{A}_\varphi^{(SE)}(m, p; r, k) &= \Delta \tilde{q}_S(m, p; k) \tilde{A}_{\varphi h}^{(1)}(r, k) \\ &- \sum_{n=0}^{\infty} \psi_A(n, r) \int_{R_1}^{R_0} dr_1 r_1 \psi_A(n, r_1) \psi_Q(m, r_1) \frac{\psi_{S_2}(p, k) \exp(k^2/4\alpha^2)}{k^2 - \lambda_A(n)}, \\ &m = 0, 1, 2, \dots, \quad p = 1, 3, 5, \dots, \end{aligned} \tag{154}$$

where the first term on the r. h. s. is from (120), (121), and the last one is derived from (55). If (153) is substituted into (138), $\Phi^{(S)}(r, k)$ becomes decomposed according to

$$\Phi^{(S)}(r, k) = \sum_{m=0}^{\infty} \sum_{p=0}^{p_1} s_2(m, p) \Phi^{(SE)}(m, p; r, k), \tag{155}$$

$$\Phi^{(SE)}(m, p; r, k) = -2 \exp\left(-\frac{k^2}{4\alpha^2}\right) k^2 \tilde{A}_\varphi^{(SE)}(m, p; r, k). \tag{156}$$

The decomposition (155) can be traced back to (84) and (139), which results in the decomposition

$$\tilde{F}_{2h}^{(S)}(m, k) = \sum_{m_1=0}^{\infty} \sum_{q=0}^{p_1} s_2(m_1, q) \tilde{F}_{2h}^{(SE)}(m; m_1, q; k), \tag{157}$$

where $\tilde{F}_{2h}^{(SE)}(m; m_1, q; k) = 0$ for even q . If (153) is substituted into (142), $\tilde{F}_{hp}^{(S)}(m, k)$ decays, in the same way, in superposed contributions according to

$$\tilde{F}_{hp}^{(S)}(m, k) = \sum_{m_1=0}^{\infty} \sum_{q=0}^{p_1} s_2(m_1, q) \tilde{F}_{hp}^{(SE)}(m; m_1, q; k), \tag{158}$$

$$\begin{aligned} &\tilde{F}_{hp}^{(SE)}(m; m_1, q; k) \\ &= \int_{R_1}^{R_0} dr r \psi_Q(m, r) \exp\left(-\frac{k^2}{4\alpha^2}\right) \left(\frac{1}{\alpha^2} - 2\frac{\partial^2}{\partial k^2}\right) k^2 \tilde{A}_\varphi^{(SE)}(m_1, q; r, k). \end{aligned} \tag{159}$$

Thus, we find the wanted decomposition of $\tilde{F}_2^{(S)}(m, k)$, substituting (157) and (158) into (145):

$$\tilde{F}_2^{(S)}(m, k) = \sum_{m_1=0}^{\infty} \sum_{q=0}^{p_1} s_2(m_1, q) \tilde{F}_2^{(SE)}(m; m_1, q; k), \tag{160}$$

$$\tilde{F}_2^{(SE)}(m; m_1, q; k) = \tilde{F}_{2h}^{(SE)}(m; m_1, q; k) + \tilde{F}_{hp}^{(SE)}(m; m_1, q; k). \tag{161}$$

where $\tilde{F}_2^{(SE)}(m; m_1, q; k) = 0$ for even q .

(160) is the wanted decomposition of $\tilde{F}_2^{(S)}(m, k)$.

If the decomposed form (160) of $\tilde{F}_2^{(S)}(m, k)$ is substituted into the r. h. s. of (148), it implies the analogous decomposition of $\tilde{S}_2^{(S)}(m, k)$. We have

$$\tilde{S}_2^{(S)}(m, k) = \sum_{m_1=0}^{\infty} \sum_{q=0}^{p_1} s_2(m_1, q) \tilde{S}_2^{(SE)}(m; m_1, q; k), \tag{162}$$

where $\tilde{S}_2^{(SE)}(m; m_1, q; k)$ is uniquely determined through

$$\mathcal{L}(m) \tilde{S}_2^{(SE)}(m; m_1, q; k) = \tilde{F}_2^{(SE)}(m; m_1, q; k), \tag{163}$$

$$\lim_{k \rightarrow \pm\infty} \tilde{S}_2^{(SE)}(m; m_1, q; k) = 0, \tag{164}$$

where $\tilde{S}_2^{(SE)}(m; m_1, q; k) = 0$ for q even.

$\tilde{S}_2^{(SE)}(m; m_1, q; k)$ is determined, like (151), (152), through the ansatzes

$$\tilde{F}_2^{(SE)}(m; m_1, q; k) = \sum_{p=0}^{\infty} f_2^{(SE)}(m, p; m_1, q) \psi_{S_2}(p, k), \tag{165}$$

$$\tilde{S}_2^{(SE)}(m; m_1, q; k) = \sum_{p=0}^{\infty} s_2^{(SE)}(m, p; m_1, q) \psi_{S_2}(p, k), \tag{166}$$

$$s_2^{(SE)}(m, p; m_1, q) = f_2^{(SE)}(m, p; m_1, q) / \lambda_{S_2}(m, p). \tag{167}$$

The final step to arrive at the overall consistency of all hydrodynamic functions is the self-consistent determination of the coefficients $s_2(m, p)$ which enter the representation (98) of $\tilde{S}(r, k)$. Starting from (146), we substitute $\tilde{S}_2(m, k)$ by (89), $\tilde{S}_2^{(A)}(m, k)$ by (151), and $\tilde{S}_2^{(S)}(m, k)$ by its decomposed representation (162) together with (166). Equating the coefficients of $\psi_{S_2}(p, k)$ for each m results in the linear equation system

$$s_2(m, p) = \sum_{m_1=0}^{\infty} \sum_{q=0}^{\infty} s_2^{(SE)}(m, p; m_1, q) s_2(m_1, q) + s_2^{(A)}(m, p),$$

$$m = 0, 1, 2, \dots, \quad p = 1, 3, 5, \dots, \quad q = 1, 3, 5, \dots. \tag{168}$$

The full consistency is reached if the pressure constant p_0 is determined. At first, we note that the coefficients $s_2^{(A)}(m, p)$ depend upon p_0 , as seen tracing back to (133). This p_0 -dependence is a linear one, as concluded from further tracing back to (46). Therefore $s_2^{(A)}(m, p)$ and $s_2(m, p)$ are correctly represented writing

$$s_2^{(A)}(m, p) = s_{20}^{(A)}(m, p) + p_0 s_{21}^{(A)}(m, p), \tag{169}$$

$$s_2(m, p) = s_{20}(m, p) + p_0 s_{21}(m, p). \tag{170}$$

Thus, (168) stands for two linear equation systems to determine $s_{20}(m, p)$ and $s_{21}(m, p)$. Then the substitution of (170) in (98) implies the linear p_0 -dependence of the vorticity function according to

$$\begin{aligned} \tilde{S}(r, k) &= \tilde{S}^{(0)}(r, k) + p_0 \tilde{S}^{(1)}(r, k) \\ &= \sum_{m=0}^{\infty} \psi_Q(m, r) \sum_{p=0}^{\infty} [s_{20}(m, p) + p_0 s_{21}(m, p)] \psi_{S_2}(p, k) \exp(k^2 / 4\alpha^2). \end{aligned} \tag{171}$$

Secondly, the limiting value $\Delta\tilde{p}_1(R_0, 0)$ given by (131) depends upon the vorticity function, which implies the linear dependence of $\Delta\tilde{p}_1(R_0, 0)$ upon p_0 . Observing (171), we rewrite (131)

$$\begin{aligned} \Delta\tilde{p}_1(R_0, 0, p_0) &= \Delta\tilde{p}_{10}(R_0, 0) + p_0 \cdot \Delta\tilde{p}_{11}(R_0, 0) \\ &= 2\alpha^2 \frac{(\sqrt{\pi}/\alpha) \log(R_0/R_1) \cdot R_0 R_1 / (R_0 - R_1) + i \lim_{k \rightarrow 0} \int_{R_1}^{R_0} dr (\partial/\partial k) \tilde{S}^{(0)}(r, k)}{1 + 2\alpha^2 \log(R_0/R_1) \cdot R_0^2 R_1^2 / (R_0^2 - R_1^2)} \\ &\quad + p_0 \cdot 2\alpha^2 \frac{i \lim_{k \rightarrow 0} \int_{R_1}^{R_0} dr (\partial/\partial k) \tilde{S}^{(1)}(r, k)}{1 + 2\alpha^2 \log(R_0/R_1) \cdot R_0^2 R_1^2 / (R_0^2 - R_1^2)}, \end{aligned} \tag{172}$$

where the evaluation follows the schema of (132).

As the third and last step, p_0 is determined through substitution of (172) into (61), i.e.,

$$C_A^+(0, \Delta\tilde{p}_{10}(R_0, 0) + p_0 \cdot \Delta\tilde{p}_{11}(R_0, 0), p_0) = \frac{1}{2} \left\{ \frac{\sqrt{\pi}}{\alpha} \left[p_0 - \frac{1}{R_0 - R_1} \right] + \left[\Delta\tilde{p}_{10}(R_0, 0) + p_0 \cdot \Delta\tilde{p}_{11}(R_0, 0) \right] \frac{R_0}{R_0 - R_1} \right\} = 0. \quad (173)$$

(173) is the detailed version of the condition (61). This condition now appears as closure relation to guarantee the consistency of all hydrodynamic functions involved.

In Figure 3a,b we present, by way of example, the characteristic axial courses of the relevant flow and stress tensor components, respectively, inside the wall, calculated according to the methods of Section 2 and 3. The underlying axial course of the reciprocal viscosity, with the same axial scale, is shown in Figure 3c.

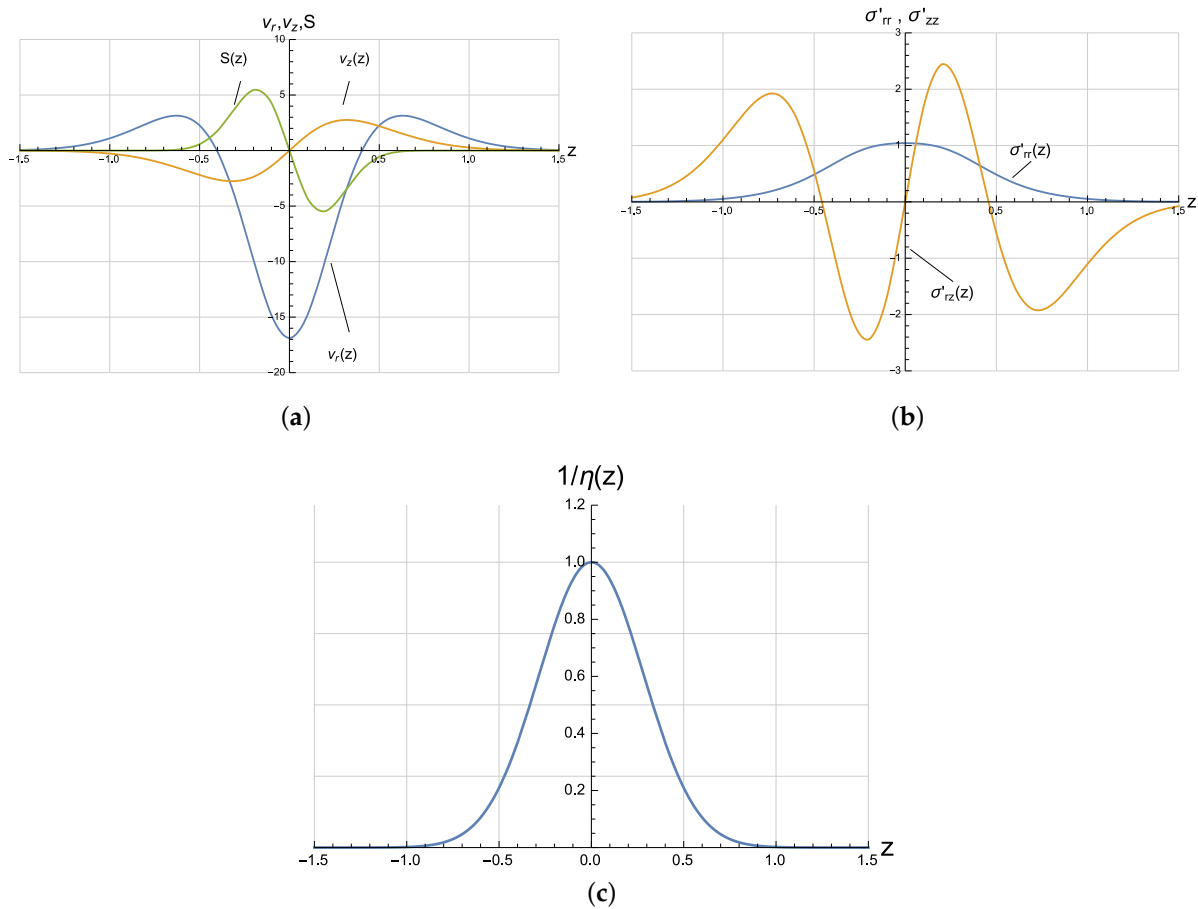


Figure 3. (a) Characteristic axial courses of the radial flow component v_r , axial flow component v_z , and vorticity function S (dimensionless coordinates and units). Calculation for $\alpha = 2.5$ (sharply peaked heating zone), $R_1 = 0.7$, and $r = 0.85$ (wall center). The change of direction of v_r on the edges of the collapsing zone is real inside the wall and no numerical artifact. (b) Characteristic axial courses of σ'_{rr} and σ'_{rz} (dimensionless coordinates and units). Calculation for $\alpha = 2.5$ (sharply peaked heating zone), $R_1 = 0.7$, and $r = 0.85$ (wall center). The hydrodynamic stress components result by multiplying with $\eta(z)$. (c) Axial course of $1/\eta(z) = \exp(-\alpha^2 z^2)$ for $\alpha = 2.5$ (sharply peaked heating zone) across the collapsing zone (dimensionless coordinates and units), as base of the courses outlined in (a,b). We further have $p_0 = 0.816$ (dimensionless), the z -mean value of $\Delta p(R_0, z) \exp(-\alpha^2 z^2)$ is 0.910 (dimensionless).

4. Collapsing Profiles and Data Evaluation

4.1. Collapsing Kinematics and Determination of the Viscosity

We are interested in the steady-state profiles of the tube boundaries due to collapsing, outlined in comoving coordinates and dimensionless quantities introduced in Section 2. The dimensionless torch velocity u (in $+z$ -direction) is

$$u = (\eta_{min}/\tau) v_T. \tag{174}$$

The steady-state axial course of the outer and inner tube radius may be denoted by $\bar{R}_0(z)$ and $\bar{R}_1(z)$, respectively. For $z \rightarrow \infty$, $\bar{R}_0(z)$ and $\bar{R}_1(z)$ approach the outer and inner tube radius R_0 and R_1 before collapsing, respectively.

In the Stokes approach, the instantaneous viscous flow is governed through the instantaneous collapsing profiles $\bar{R}_0(z)$ and $\bar{R}_1(z)$. We will assume, for a moment, that the flow components may be known for arbitrary $\bar{R}_0(z)$ and $\bar{R}_1(z)$. This fictive functional dependence may be denoted by $v_r(r, z, \{\bar{R}_0, \bar{R}_1\})$ and $v_z(r, z, \{\bar{R}_0, \bar{R}_1\})$. Then $\bar{R}_0(z)$ and $\bar{R}_1(z)$ obey the kinematic equations (see, e.g., [11])

$$d\bar{R}_i(z)/dz = -\frac{v_r(\bar{R}_i(z), z, \{\bar{R}_0(z), \bar{R}_1(z)\})}{u - v_z(\bar{R}_i(z), z, \{\bar{R}_0(z), \bar{R}_1(z)\})}, \quad i = 0, 1, \tag{175}$$

to be solved with the boundary conditions

$$\lim_{z \rightarrow \infty} \bar{R}_i(z) = R_i, \quad i = 0, 1. \tag{176}$$

In collapsing experiments, the reduction ΔR_0 of the outer tube radius and the increase ΔW of the tube wall thickness can be measured with high accuracy [9]. We have

$$\begin{aligned} \Delta R_0 &= \lim_{z \rightarrow \infty} \bar{R}_0(z) - \lim_{z \rightarrow -\infty} \bar{R}_0(z) \\ &= -\int_{-\infty}^{\infty} dz \frac{v_r(\bar{R}_0(z), z, \{\bar{R}_0(z), \bar{R}_1(z)\})}{u - v_z(\bar{R}_0(z), z, \{\bar{R}_0(z), \bar{R}_1(z)\})}, \end{aligned} \tag{177}$$

$$\Delta W = \lim_{z \rightarrow -\infty} (\bar{R}_0(z) - \bar{R}_1(z)) - (R_0 - R_1). \tag{178}$$

From Section 3, the flow components $v_r(r, z)$ and $v_z(r, z)$ are known for constant $\bar{R}_0(z) \equiv R_0$ and $\bar{R}_1(z) \equiv R_1$ (the parametric dependence upon R_0 and R_1 will be omitted in the following). Their substitution into (175) is allowed if any corrections from non-vanishing boundary inclinations $d\bar{R}_0(z)/dz$ and $d\bar{R}_1(z)/dz$ can be neglected. Because of $d\bar{R}_0(z)/dz \rightarrow 0$ and $d\bar{R}_1(z)/dz \rightarrow 0$ for $u \rightarrow \infty$, as concluded from (175), obviously, this is possible for sufficiently large u . At this point, we outline the more general result, which includes a remainder of the order of the relative error of (179) due to the neglected boundary inclination. We have

$$\Delta R_0 = -(1/u) \int_{-\infty}^{\infty} dz v_r(R_0, z) \cdot (1 + O(1/w^3 u^2)). \tag{179}$$

The remainder in (179) is governed by the dimensionless torch velocity u and the dimensionless wall thickness before collapsing $w = R_0 - R_1$. The detailed discussion is given in Section 5.

To evaluate (179) we introduce the Fourier integral representation of the total radial flow component $v_r(r, z)$

$$v_r(r, z) = (1/2\pi) \int_{-\infty}^{\infty} dk \exp(ikz) \tilde{v}_r(r, k), \tag{180}$$

where from (11), (25), and (30)

$$\tilde{v}_r(r, k) = \tilde{v}_{rh}(r, k) - i k \tilde{A}_{\phi p}(r, k). \tag{181}$$

The reverse of (180) is

$$\tilde{v}_r(r, k) = \int_{-\infty}^{\infty} dz \exp(-ikz) v_r(r, z), \tag{182}$$

so that

$$\int_{-\infty}^{\infty} dz v_r(r, z) = \lim_{k \rightarrow 0} \tilde{v}_r(r, k) = \ll v_r(r, z) \gg, \tag{183}$$

where $\ll v_r(r, z) \gg$ may abbreviate the axial overall integral of the radial flow component on the l. h. s. of (183). Then (179) yields

$$\Delta R_0 = -(1/u) \ll v_r(R_0, z) \gg \cdot (1 + O(1/w^3 u^2)). \tag{184}$$

$\ll v_r(r, z) \gg$ can be represented combining (181), (43), (44) and (55), with regarding the constraint (61). We arrive at

$$\ll v_r(r, z) \gg = -(1/r) \lim_{k \rightarrow 0} C_A^{(-)}(k, \Delta \tilde{p}_1(R_0, k)). \tag{185}$$

(185) can be further evaluated observing (45) and (173) so that an almost closed representation in terms of experimental input parameters is reached. We find

$$\begin{aligned} & \ll v_r(r, z) \gg \\ &= -(1/r) \left\{ \frac{\sqrt{\pi}}{\alpha} \frac{R_0 R_1}{2(R_0 - R_1)} - \left[\Delta \tilde{p}_{10}(R_0, 0) + p_0 \cdot \Delta \tilde{p}_{11}(R_0, 0) \right] \frac{R_0^2 R_1^2}{2(R_0^2 - R_1^2)} \right\}, \end{aligned} \tag{186}$$

where $\Delta \tilde{p}_{10}(R_0, 0)$ and $\Delta \tilde{p}_{11}(R_0, 0)$ are given by (172), and the constant pressure contribution p_0 is determined through (173).

The formulae (184) to (186) represent the main result of our analysis. Because no closed analytic expressions are available, we summarize for practical applications (dimensionless units)

$$\Delta R_0 = \frac{1}{u} \frac{\sqrt{\pi}}{\alpha} \frac{R_1}{2(R_0 - R_1)} \cdot \text{Fac}(R_1/R_0, \alpha) \cdot (1 + O(1/w^3 u^2)). \tag{187}$$

The three factors on the r. h. s. of (187) stand for the successive improvement of the collapsing theory. The first factor corresponds to the earlier result of the asymptotic 1D and 2D theory [11]. The second one summarizes the corrections resulting from the strong analysis of this work. Characteristic courses of the correction factor $\text{Fac}(R_1/R_0, \alpha)$ are shown in Figure 4, and analytic approximants of $\text{Fac}(R_1/R_0, \alpha)$ (relative accuracy $\leq 10^{-3}$) are outlined in Appendix D. The remainder involved in the third factor comes from (179) and estimates the relative error if (187) is applied beyond the asymptotic limit $u \rightarrow \infty$ (see Section 5). For sufficiently large u where the remainder in (187) can be neglected, $\Delta R_0 \cdot u$ only depends upon geometry parameters entering the r. h. s. of (187). This dependence, rewritten in SI units, is plotted in Figure 5 for different R_1/R_0 . The correction factor $\text{Fac}(R_1/R_0, \alpha)$ was first introduced in [9] (therein denoted as the F-factor) to quantify the deviations of actual FEM calculations from the 1D theory.

Based on (187), an adequate relation for ΔW exists in virtue of the principle of local mass conservation far from the collapsing region [11] according to

$$\Delta W = (\sqrt{\pi}/2\alpha u) \cdot \text{Fac}(R_1/R_0, \alpha) \cdot (1 + O(1/w^3 u^2)). \tag{188}$$

We will abandon the detailed calculation of the courses $\bar{R}_0(z)$ and $\bar{R}_1(z)$. The evaluation shows that in practice, $\bar{R}_0(z)$ equals its limiting values for $z \rightarrow \pm\infty$ for axial distances $|z| \gg (\alpha^2(R_0 - R_1))^{-1}$ from the temperature peak. This is the condition to measure ΔR_0 and ΔW with a sufficient accuracy, too.

The minimum viscosity η_{min} according to the maximum tube temperature T_{max} of the heating zone is implicitly involved in the dimensionless torch velocity u given by (174). Changing to SI units and observing (8), we find from (187)

$$\eta_{min} = \frac{\sqrt{\pi}}{2} \cdot \frac{\tau \Delta z_e}{v_T \Delta R_0} \cdot \frac{R_1}{W} \cdot \text{Fac}\left(\frac{R_1}{R_0}, \frac{R_0}{\Delta z_e}\right) \cdot (1 + O(1/w^3 u^2)), \tag{189}$$

where $W = R_0 - R_1$. The half-width Δz_e of the axial viscosity course according to (6) must be fitted from the measured axial temperature course based on appropriate model relations describing the temperature-dependent viscosity of molten glasses, as discussed in Section 1.

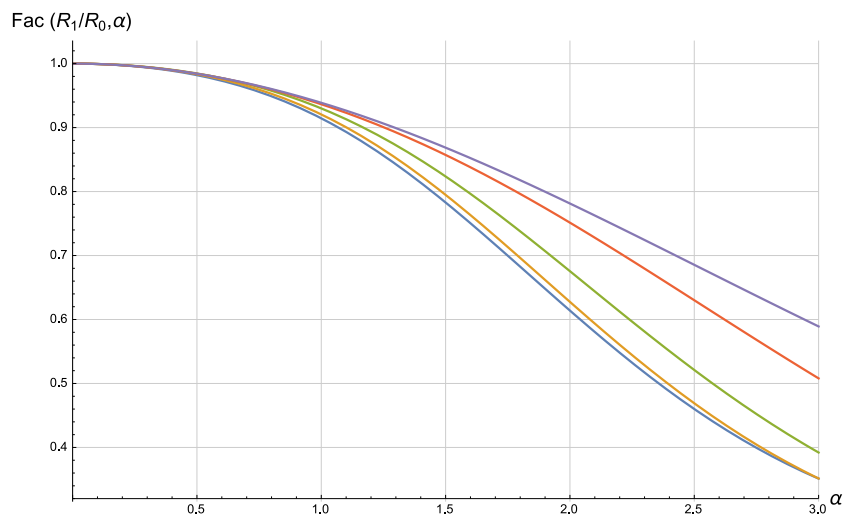


Figure 4. Correction factor $\text{Fac}(R_1/R_0, \alpha)$ versus α , according to Equations (187) and (188), for $R_1/R_0 = 0.6, 0.7, 0.8, 0.9, 0.95$ (from below).

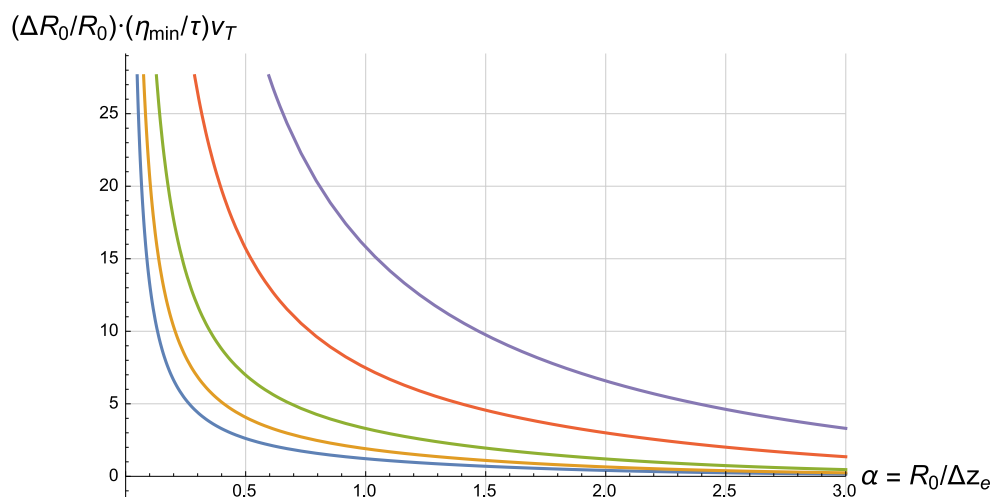


Figure 5. Dependence of the reduction ΔR_0 of the outer tube radius upon the half-width Δz_e of the axial reciprocal viscosity course for large torch velocities. Plots for $R_1/R_0 = 0.6, 0.7, 0.8, 0.9, 0.95$ (from below). R_0, R_1 outer and inner tube radius, respectively, before collapsing, η_{min} minimum viscosity, τ surface tension, v_T torch velocity. All quantities in SI units.

4.2. Suppression of Collapsing and Measuring of Surface Tensions

The contactless measuring of the surface tension τ of molten glasses through collapsing has been first described in [9] in detail. The principle can be understood as modification of the well-known bubble pressure method to determine τ (see, e.g., [22]). The data analysis outlined in [9] to determine τ is a refined version of the 1D theory. We will point out that the hydrodynamic theory predicts “hydrostatic” conditions which allow the measurement of τ without the knowledge of details of the viscosity courses across the collapsing zone, as well as without the knowledge of details of the hydrodynamic theory at all.

We focus on an axial tube region closely around the temperature peak, and provide that the surface tension τ of molten glasses can be assumed as constant for the corresponding temperature interval. We again consider a collapsing tube with sufficiently small boundary inclinations $d\bar{R}_0(z)/dz$ and $d\bar{R}_1(z)/dz$. Then the (dimensionless) normal forces induced by the surface tension at the outer and inner surface are independent of z and equal to $-1/R_0$ and $1/R_1$, respectively. The force balance at the boundaries becomes disturbed if an additional “hollow”-pressure p_h in the hollow space $r < R_1$ of the tube, and quite similarly, if an additional, external “torch”-pressure p_T in the exterior of the tube $r > R_0$ is applied. Both of them will cause a disturbing normal force at the adjacent boundary against the normal direction, which may be assumed as independent of z (at least across the collapsing zone). Thus, the surface tension-induced normal force at the outer and inner boundary must be substituted by $-1/R_0 - p_T$ and $1/R_1 - p_h$, respectively, to be denoted as the disturbed normal forces in the following. In [9], this substitution is introduced into the 1D- theory, and τ is determined through extrapolation from collapsing data for different R_0 and R_1 .

Obviously, the viscous flow and therefore, the collapsing must expire if the disturbed normal forces on both the boundaries become equal, i.e., for

$$-1/R_0 - p_T = 1/R_1 - p_h. \tag{190}$$

If (190) is satisfied, the constant pressure p_0 inside the tube will solely balance the disturbed normal forces on both the boundaries. This implies, at the same time, the absence of the viscous flow, so that neither a tangential force at the boundaries, nor a hydrodynamic pressure contribution will exist. Both p_h and p_T can be involved into the general formalism outlined in Sections 2 and 3. In doing so, $\Delta p(R_0, z)$ has to be substituted by $\Delta p(R_0, z) + \Delta p_{ex}$ for $r = R_0$ in (23), where $\Delta p_{ex} = p_h - p_T$, meanwhile there remains $\Delta p(R_1, z) = 0$ for $r = R_1$. The step by step analysis shows that the viscous flow becomes expired, in accordance with (190), if $\Delta p(R_0, z)$ reaches the critical value

$$\Delta p_{ex} = \Delta p_{Cex} = (R_0 + R_1)/R_0R_1. \tag{191}$$

Changing to SI units, the surface tension τ follows from (191) according to

$$\tau = \Delta p_{Cex}R_0R_1/(R_0 + R_1). \tag{192}$$

In practice, Δp_{Cex} may be determined through successive change of Δp_{ex} and extrapolation to zero reduction $\Delta R_0 \rightarrow 0$, where the precondition of negligible boundary inclinations is satisfied.

5. Discussion

5.1. General

We discuss three aspects. First, there is the problem of validity of our results if applied to torch velocities u where the precondition of the asymptotic limit $u \rightarrow \infty$ is not well satisfied. Available analytic methods allow, at least, an error estimation of the results of Section 3, if taking into account the effect of the boundary inclination. Using the principles of AMSA outlined and discussed in detail, e.g., in [11], the geometry parameters R_0 and R_1 are considered to be no longer constant, but slightly dependent upon the “slow” axial

variable $Z = \varepsilon z$, $\varepsilon \ll 1$. This implies the substitution of $\partial/\partial z$ by $\partial/\partial z + \varepsilon\partial/\partial Z$, as the base of a perturbation treatment of the hydrodynamic equations, boundary conditions, and kinematic equations in powers of ε . Then the kinematic equations specify $\varepsilon = 1/wu$. For symmetry reasons, the lowest-order correction to ΔR_0 as outlined in (179) and (187) results in the order ε^2 .

Secondly, the correction factor $\text{Fac}(R_1/R_0, \alpha)$ in (187) and (188) outlined in Appendix D and plotted in Figure 4 quantifies the deviation of the established zeroth and first-order asymptotic analysis of collapsing (1D- and 2D-theory [11]) from the exact analytic theory. $\text{Fac}(R_1/R_0, \alpha)$ monotonously decreases with α from unity for $\alpha = 0$ to the order 10^{-1} for $\alpha > 1$. These findings are in accordance with error estimations given within the frame of the 1D and 2D-theory [11], where the breakdown of the asymptotic analysis for $\alpha \rightarrow 1$ is predicted. Remarkably, FEM results for $0 \leq \alpha \leq 1$ outlined in [11], too, as well as FEM results for $\alpha > 1$ reported in [9] do not well agree with (187) for $\alpha > 1/2$. In particular, the correction factor calculated from FEM should much weaker decrease for $\alpha > 1/2$, compared with our strong analytic results. This discrepancy is open for discussion. The reason may be an inappropriate FEM algorithm in treating axial boundary conditions ad infinity, where $\eta(z)$ increases beyond all limits.

We see from (186) that the correction factor $\text{Fac}(R_1/R_0, \alpha)$ is related to the hydrodynamic pressure contribution $\Delta p(R_0, z)$ only. The latter, on its part, is induced through the axial viscosity dependence only. In this context, we note that $\Delta p(R_0, z)$ vanishes for $\alpha \rightarrow 0$ where boundary condition (23) of the normal force balance is solved for $\Delta p(R_0, z) = 0$ (see [11], Section 3.1). $\text{Fac}(R_1/R_0, \alpha)$ decreases $\propto \alpha^2$ for small α . This is a second-order effect in α , which is not accessible in zeroth and first perturbation order of AMSA (1D and 2D theory [11]) where $\Delta p(R_0, z)$ is not involved. The hydrodynamic pressure contribution $\Delta p(R_0, z)$ acts against the surface tension. Therefore, the collapsing efficiency becomes diminished for increasing α , compared to the predictions of the 1D and 2D-theory.

To evaluate experimental data, on the other hand, the formulae from the 1D-theory represent a very convenient framework to calculate the minimum viscosity along the axial viscosity course, which corresponds to the maximum temperature of the heating zone [9]. This advantage also persists if working with the correct formulae (187) to (189). Thus, the minimum viscosity η_{min1D} calculated from the 1D-theory must be corrected to $\eta_{min} = \eta_{min1D} \cdot \text{Fac}(R_1/R_0, \alpha)$ (see also [9]), provided the preconditions of (184) hold true. In other words, the data evaluation according to the 1D-theory involves a systematic error so that the minimum viscosity attributed to the maximum temperature is calculated to be *too large* in comparison to the reality. Regarding the range of $\text{Fac}(R_1/R_0, \alpha)$, the actual temperature-dependent viscosity data may be smaller up to one order of magnitude compared with the data evaluated by means of the 1D-theory.

The third aspect concerns the question how our theoretical results are changed if the viscosity course in axial and radial direction does not completely meet the preconditions of our theory. We will first assume that the temperature measured at the external tube boundary indeed equals the temperature across the tube wall, so that a radial viscosity dependence does not occur, but $1/\eta(z)$ may deviate from the Gaussian model course (6). This is a typical problem to be answered through AMSA [11].

We provide dimensionless quantities and coordinates. If $1/\eta(z)$ deviates from the Gaussian model course, AMSA shows that the prefactor $\sqrt{\pi}/\alpha$ in (187) and (188) must be substituted by $\int_{-\infty}^{\infty} dz/\eta(z)$, where $1/\eta(z)$ is the reciprocal viscosity course, back-calculated from experimental temperature data and normalized to the maximum value unity. This suggests an extension to sharply peaked, non-Gaussian $1/\eta(z)$ -profiles where the model parameter α must be chosen such that

$$\int_{-\infty}^{\infty} dz \left(\delta(1/\eta(z)) \right)^2 = \int_{-\infty}^{\infty} dz \left(1/\eta(z) - \exp(-\alpha(z - z_0)) \right)^2 = \text{Min!}, \quad (193)$$

looking for the minimum with respect to α and z_0 . Because (193) also implies $\int_{-\infty}^{\infty} dz \delta(1/\eta(z)) = 0$, the principles of AMSA predict a second-order correction only, which results in relative corrections of ΔR_0 and ΔW of the order $O((\alpha^2/\pi) \int_{-\infty}^{\infty} dz (\delta(1/\eta(z)))^2)$.

A more serious problem arises if the axial temperature course measured at the outer tube boundary does not exactly represent the temperature distribution inside the tube wall. In particular, the heat flux from the torch passing the outer tube boundary and flowing through the tube wall away from the heating zone creates a positive radial temperature gradient near the torch. In addition, convective effects due to the torch motion cause a distortion of the comoving temperature field inside the tube wall, leading to an enhancement of this radial temperature gradient. Because the viscosity increases with decreasing temperature, a viscosity measurement which evaluates the surface temperature only and neglects the positive radial temperature gradient would result in a *higher* viscosity assigned to the measured maximum temperature, compared to the reality. Superposed thermal radiation effects have been earlier discussed for slender geometries [23]. It has been concluded therein that the thermal radiation would increase the effective thermal conductivity of molten glasses by a factor of about 3 and reduce the systematic error due to heat conduction. Tube geometries as here described, sharply peaked temperature profiles and peak temperatures at least up to about 2200 K provided, exact solutions of the convective heat conduction equation and the integral equation of thermal radiation (Th. Klupsch, unpublished) show that the energy transport via heat conduction strongly dominates the superposed thermal radiation.

To estimate the systematic error in viscosity measurements caused by heat conduction, we briefly report on model calculations (Th. Klupsch, unpublished) on the convective heat transport within the wall of infinitely extended tubes, assuming a prescribed temperature course at the *outer* boundary $r = R_0$ in comoving dimensionless coordinates according to

$$T(z) = (T_{max} - T_{\infty}) \exp(-z^2/\Delta z_{Te}^2) + T_{\infty}, \tag{194}$$

and a vanishing radial heat flux at the inner boundary $r = R_1$. $2\Delta z_{Te}$ is the axial $1/e$ -width of the temperature peak at the outer boundary, and T_{max} , and T_{∞} now denote the peak temperature at the outer boundary, and the room temperature, respectively. The maximum temperature difference ΔT between opposite points in radial direction at the outer and inner boundary can be roughly estimated to (in SI units)

$$\Delta T/(T_{max} - T_{\infty}) \approx (W/\Delta z_{Te}) \cdot 1.66 \cdot 10^{-2}, \text{ if } v_T/\kappa < 1 \cdot 10^2 \text{ m}^{-1}, \tag{195}$$

$$\Delta T/(T_{max} - T_{\infty}) \approx (W/\Delta z_{Te}) \cdot (v_T/\kappa) \cdot 1.66 \cdot 10^{-4} \text{ m}, \text{ if } v_T/\kappa > 1 \cdot 10^2 \text{ m}^{-1}, \tag{196}$$

where $\kappa = 0.9 \cdot 10^{-6} \text{ m}^2/\text{s}$ is the temperature conductivity of molten glasses [21]. The threshold $v_T/\kappa = 1 \cdot 10^2 \text{ m}^{-1}$ characterizes the transition to a dominating convective heat transport. The axial viscosity model course $\eta_{mod}(z)$ at the outer boundary $r = R_0$ (corresponding to (6)) may be derived from the empirical relation of the temperature-dependent viscosity of molten glasses (silica) [11]

$$\eta_{emp}(T) = \exp(-18.77 + 66420/T) \tag{197}$$

(η_{emp} in Pa s, T in K), so that $\eta_{mod}(z)$ follows substituting (194) into (197). For $T_0 = 2200$ K, $T_{\infty} = 300$ K, and $\Delta z_{Te} = 2$ (dimensionless) corresponding to $R_0 = 1 \cdot 10^{-2}$ m and $\Delta z_{Te} = 2 \cdot 10^{-2}$ m, the minimum value of $\eta_{mod}(z)$ is $\eta_{min} = 9.1 \cdot 10^4$ Pa s, and (193) yields $\alpha = 2.6$. The radial temperature gradient will cause the uncertainty $\Delta\eta_{min}$ of the η_{min} -value attributed to the maximum temperature T_0 at the outer boundary. From (197), this systematic error in viscosity measurements caused by heat conduction is roughly estimated to

$$|\Delta \log \eta_{min} / \log \eta_{min}| \approx \Delta T / (T_{max} - T_{\infty}). \tag{198}$$

5.2. Optimizing Experimental Conditions

We will discuss arrangements which meet the requirements of our theory, as precondition to arrive at a correct data evaluation. We are interested, in addition, in conditions to minimize accompanying errors, which is necessary to estimate an accuracy limit of viscosity measurements through collapsing. According to our original motivation, we will focus on equipment using sharply peaked axial temperature courses. From viewpoint of the hydrodynamic theory, the accuracy of the viscosity, if back-calculated from collapsing data, is in any case limited through the neglected boundary inclination. The order of this relative error is given by the remainders of (187) and (188). Provided that the data evaluation is based on the formulae (187) and (188) we will exclusively look for arrangements where the relative error due to the neglected boundary inclination does not exceed a prescribed limit. This *mandatory* error limit may be denoted by $Erhy$. Keeping $w = R_0 - R_1$ fixed, $Erhy = 1/u^2w^3$ determines a minimum dimensionless torch velocity u_{min} which at least must be applied. Thus, measurements have been carried out for the precondition

$$u \geq u_{min} = 1/Erhy^{1/2}w^{3/2}. \tag{199}$$

According to (187) and (188), both the collapsing-relevant parameter ΔR_0 as well as ΔW drop down for increasing u . Substituting (199) in (187) and (188), we see that in any case, the experimental tools must be arranged such that both ΔR_0 and ΔW (both in dimensionless units) must not exceed a maximum value according to

$$\Delta R_0 \leq Erhy^{1/2}w^{1/2}(1-w)(\sqrt{\pi}/2\alpha)Fac(R_1/R_0, \alpha), \tag{200}$$

$$\Delta W \leq Erhy^{1/2}w^{3/2}(\sqrt{\pi}/2\alpha)Fac(R_1/R_0, \alpha). \tag{201}$$

We note that $w^{1/2}(1-w)$ assumes its maximum 0.385 at $w = 0.33$, and ΔW overcomes ΔR_0 for $w > 0.5$.

In continuing with the numerical example of Section 5.1, we prescribe $Erhy = 1 \cdot 10^{-1}$ and $w = 0.33$, so that $Erhy^{1/2}w^{1/2}(1-w) = 0.12$, $Erhy^{1/2}w^{3/2} = 0.06$, and $(\sqrt{\pi}/2\alpha)Fac(R_1/R_0, \alpha) = 0.15$ for $\alpha = 2.6$. This provided, the tolerable range of ΔR_0 and ΔW according to (200) and (201) is restricted to $\Delta R_0 \leq 1.9 \cdot 10^{-2}$ and $\Delta W \leq 9.2 \cdot 10^{-3}$, respectively.

In SI units, this result can be summarized as follows: Continuing the numerical example at the end of Section 5.1, we consider a tube with the outer radius $1 \cdot 10^{-2}$ m and the thickness $W = w \cdot 1 \cdot 10^{-2} = 3.3 \cdot 10^{-3}$ m before collapsing. Then the collapsing equipment must be arranged such that the reduction ΔR_0 of the external tube radius does not exceed $1.9 \cdot 10^{-4}$ m, and the increasing ΔW of the wall thickness does not exceed $9.2 \cdot 10^{-5}$ m, respectively. This provided, the preconditions are satisfied to evaluate the experimental data, applying (187) or (188), with a relative accuracy of about ten percent. The permissible range of the dimensionless torch velocity is $u \geq 1.67 \cdot 10^1$. For a surface tension of molten glasses $\tau = 4 \cdot 10^{-1}$ Pa · m [21,22], the torch velocity in SI units must satisfy the restriction $v_T = u \cdot \tau/\eta_{min} \geq 7.3 \cdot 10^{-5}$ m/s. We note that, of course, both ΔR_0 and ΔW assume their permitted maximum if the minimum torch velocity is applied. From $W/\Delta z_{Te} = 0.16$ and $v_T/\kappa \geq 8.1 \cdot 10^1 \text{ m}^{-1}$ we find, according to (195), $\Delta T/(T_{max} - T_\infty) \geq 3 \cdot 10^{-3}$ for the entire range of the permitted torch velocity, where the minimum is assumed for the minimum torch velocity. This means that, applying the permitted minimum torch velocity, the mandated relative error $Erhy = 1 \cdot 10^{-1}$ for data evaluation overcomes the collateral error through heat conduction. This also means that the general precondition of our theory, namely to neglect a radial viscosity dependence is acceptable.

The numerical example outlined above shows that despite the provided ten percent order of $Erhy$, the measurement of the relevant geometry parameter, in particular, the change of the outer tube radius and wall thickness, respectively, would require a considerable accuracy [9]. Such a requirement could be substantially reduced choosing larger widths of the axial temperature peak. If Δz_{Te} is doubled to $\Delta z_{Te} = 4$ (dimensionless),

corresponding to $4 \cdot 10^{-2}$ m, but keeping other parameters fixed, we get $\alpha = 1.3$ and $(\sqrt{\pi}/2\alpha)\text{Fac}(R_1/R_0, \alpha) = 0.59$, and the permitted range of ΔR_0 and ΔW would increase by a factor 4 to (in SI units) $\Delta R_0 \leq 7.2 \cdot 10^{-4}$ m and $\Delta W \leq 3.5 \cdot 10^{-4}$ m, respectively. In addition, the relative error through heat conduction on the entire range of the permitted torch velocity would be reduced according to $\Delta T/(T_{max} - T_{\infty}) \geq 1.4 \cdot 10^{-3}$. That means that for both the numerical examples considered the error through heat conduction is negligible if working with the minimum permitted torch velocity, and at the same time, the basic premise to deal with an only z -dependent viscosity is justified in turn. The collateral error through heat conduction may arrive at the ten percent range if torch velocities v_T of the order 10^{-3} m/s would be necessary to get acceptable collapsing efficiencies. This is the case, according to (174), if η_{min} approaches or falls below the order 10^3 Pa s. Regarding the extreme temperature dependence of the glass viscosity, this may be realistic for peak temperatures exceeding 2200 K.

6. Summary

We improve the theoretical base to understand collapsing of glass tubes, as necessary precondition to establish the steady-state collapsing with moving torch as a precise and contact-free method to determine temperature-dependent viscosities and surface tensions of molten glasses. We focus, in particular, on novel analytical solutions of the covering boundary value problem of the Stokes equation for sharply peaked axial courses of the reciprocal viscosity. Our aim is to extend the validity range beyond the limits of the established asymptotic methods (AMSA). The strong solutions derived here neglect the inclinations of the tube boundaries, which meets the conditions of the collapsing kinematics for sufficiently large torch velocities. We take up the ideas of AMSA to estimate the order of the corrections, if the boundary inclination should be taken into account.

Despite the neglected boundary inclination, the presupposed strong axial viscosity dependence leads to a substantial complication of the boundary value problem. For disentanglement, we derive a gradually interdependent hierarchy of equations and boundary conditions for the stream function, the vorticity and pressure, starting from the experimental input conditions. In addition, we introduce axial Fourier transforms to set up of solutions for infinitely extended tubes, which obey axial boundary conditions according to the expiring viscous flow behavior for unboundedly increasing viscosity courses beyond the collapsing zone. We outline model solutions for the course of the reciprocal viscosity specified as Gaussians, the axial half-width of which may be much smaller than the outer tube radius.

We show that for sufficiently sharply peaked axial temperature courses, a connection exists between the steepness of the axial course of reciprocal viscosity, the vorticity of the viscous flow, and the radial pressure gradient. The latter acts against the surface tension and retards the collapsing kinematics. This effect is not predicted by the established asymptotic theory. Thus, the minimum viscosity attributed to the peak temperature, if evaluated from experimental data according to the asymptotic 1D and 2D theory, is found to be too large up to one order of magnitude.

For data evaluation in practice, in particular, for the back-calculation of the viscosity from experimental input data, we outline a simple extension of convenient formulae from the 1D theory in virtue of a correction factor only. In addition, we outline error estimations regarding both the unavoidable boundary inclination and convective heat conduction within the tube wall. Both systematic errors will work against each other, if the torch velocity is considered to be a run parameter. But model calculations predict the existence of a reasonable compromise.

Funding: This research received no external funding.

Acknowledgments: The author thanks his former colleague J. Kirchhof from the Department of Fiber Optics, Leibniz Institute of Photonic Technologies in Jena, Germany for his suggestion to deal with the hydrodynamic theory of collapsing, and all former colleagues for support and critical discussions.

Conflicts of Interest: The author declares no conflict of interest.

Appendix A. Solution of Certain Differential Equations

Operating with Fourier transforms, boundary value problems of ordinary differential equations for r -dependent functions have to be solved, as seen, e.g., by (36) to (38), where the Fourier variable k appears as parameter. Because the closed solution in terms of cylinder functions is intransparent, we look for a solution as series expansion in r and meromorphic function of k . We consider as prototype the boundary value problem

$$(\mathcal{D}_r - k^2)y_h(r, k) = 0, \tag{A1}$$

$$(d/dr)y_h(r, k)|_{r=R_0} = f_0(k), (d/dr)y_h(r, k)|_{r=R_1} = f_1(k). \tag{A2}$$

We solve (A1), (A2) as series expansion in terms of $\psi_A(n, r)$ with k -dependent coefficients where poles appear at the imaginary k -axis. Obviously, $y_h(r, k)$ is solution of the integral equation

$$y_h(r, k) = y_0(r, k) + k^2 \int_{R_1}^{R_0} dr_1 G_0(r, r_1)y_h(r_1, k), \tag{A3}$$

where $y_0(r)$ is solution of

$$\mathcal{D}_r y_0(r, k) = 0 \tag{A4}$$

with the boundary conditions (A2), and $G_0(r, r_1)$ is the Greens function of the operator \mathcal{D}_r , which obeys

$$\mathcal{D}_r G_0(r, r_1) = \delta(r - r_1) \tag{A5}$$

with the homogeneous boundary conditions

$$(d/dr)G_0(r, r_1)|_{r=R_0} = 0, (d/dr)G_0(r, r_1)|_{r=R_1} = 0. \tag{A6}$$

$G_0(r, r_1)$ is represented in terms of $\psi_A(n, r)$ and $\lambda_A(n)$, introduced by (39) to (41), according to

$$G_0(r, r_1) = \sum_{n=0}^{\infty} \psi_A(n, r)r_1\psi_A(n, r_1)/\lambda_A(n). \tag{A7}$$

$y_0(r, k)$ is explicitly given by

$$y_0(r, k) = c^{(-)}(k) \cdot (-1/r) + c^{(+)}(k) \cdot r, \tag{A8}$$

$$c^{(-)}(k) = -(f_0(k) - f_1(k))R_0^2R_1^2/(R_0^2 - R_1^2), \tag{A9}$$

$$c^{(+)}(k) = (f_0(k)R_0^2 - f_1(k)R_1^2)/(R_0^2 - R_1^2). \tag{A10}$$

The series expansion of $y_0(r, k)$ in terms of $\psi_A(n, r)$ according to (47) yields

$$y_0(r, k) = \sum_{n=0}^{\infty} \psi_A(n, r)\beta(n, k), \beta(n, k) = c^{(-)}(k)\beta_A^-(n) + c^{(+)}(k)\beta_A^+(n). \tag{A11}$$

Substituting (A7) and (A11) into (A3), and applying (39), we arrive at

$$y_h(r, k) = - \sum_{n=0}^{\infty} \psi_A(n, r) \frac{\beta(n, k)\lambda_A(n)}{k^2 - \lambda_A(n)}. \tag{A12}$$

The particular solution $y_p(r, k)$ of the ordinary inhomogeneous differential equation

$$(\mathcal{D}_r - k^2)y_p(r, k) = g(r, k) \tag{A13}$$

with homogeneous boundary condition

$$(d/dr)y_p(r,k)|_{r=R_0} = 0, (d/dr)y_p(r,k)|_{r=R_1} = 0 \tag{A14}$$

is given by

$$y_p(r,k) = \int_{R_1}^{R_0} dr_1 G(r,r_1,k) g(r_1,k). \tag{A15}$$

$G(r,r_1,k)$ is the Greens function of the operator on the l. h. s. of (A13), according to

$$(\mathcal{D}_r - k^2) G(r,r_1,k) = \delta(r - r_1), \tag{A16}$$

which satisfies homogeneous boundary conditions according to (A6). The direct ansatz yields

$$G(r,r_1,k) = - \sum_{n=0}^{\infty} \psi_A(n,r) r_1 \psi_A(n,r_1) / (k^2 - \lambda_A(n)). \tag{A17}$$

$y_h(r,k)$ as well as $y_p(r,k)$ are represented as meromorphic functions of k (for convergence, see Appendix C). Because of $\lambda_A(n) < 0$, all poles are on the imaginary k -axis, beside the path of the k -integration along the real k -axis. The orthonormal base, in the present case $\psi_A(n,r), n = 0, 1, 2, \dots$, must be chosen in any case in accordance with the boundary conditions to be satisfied by the Greens functions $G_0(r,r_1)$ and $G(r,r_1,k)$. In this respect, the boundary conditions of $y_0(r,k)$ are irrelevant because, regarding the expansions (A11), each continuous function can be approached through any complete orthonormal base in $R_1 \leq r \leq R_0$ with arbitrary accuracy in the quadratic mean.

Appendix B. Derivation of (76)

As outlined in Section 3.2, the solution $\tilde{S}(r,k)$ of (62) which satisfies the radial boundary condition (63) can be attributed to the solution of two sets of inhomogeneous ordinary differential Equations (75) and (76). Meanwhile the mathematical steps are straightforwardly carried out for the particular solution $\tilde{S}_p(r,k)$ of (62), we must use the methods of Appendix A to derive a similar equation set for the homogenous solution $\tilde{S}_h(r,k)$ of (62).

We first interchange the order of separation and substitution, as outlined in Section 3.2, and start with the substitution

$$\tilde{S}_h(r,k) = \exp(k^2/4\alpha^2) \tilde{S}_{hs}(r,k), \tag{A18}$$

where $\tilde{S}_{hs}(r,k)$ obeys the differential equation

$$\mathcal{D}_r \tilde{S}_{hs}(r,k) = (4\alpha^2 + 2k^2 - 4\alpha^4 \partial^2 / \partial k^2) \tilde{S}_{hs}(r,k), \tag{A19}$$

to be solved with the boundary condition

$$\tilde{S}_{hs}(r,k) = 2 \exp(-k^2/4\alpha^2) \mathcal{D}_r \tilde{A}_\varphi(r,k) \text{ at } r = R_0, R_1. \tag{A20}$$

The r. h. s. of (A19) and (A20) may be denoted by

$$\tilde{F}_{hs}(r,k) = (4\alpha^2 + 2k^2 - 4\alpha^4 \partial^2 / \partial k^2) \tilde{S}_{hs}(r,k), \tag{A21}$$

$$\Phi(r,k, \Delta p_1(R_0,k), p_0) = 2 \mathcal{D}_r \tilde{A}_\varphi(r,k), \tag{A22}$$

respectively, where $\Phi(r,k, \Delta p_1(R_0,k), p_0)$ is outlined by (87). Both the functions may be considered, for a moment, to be arbitrary functions depending upon r and the arbitrary parameter k . Then (A19) is an ordinary inhomogeneous differential equation with respect

to r , to be solved with the boundary condition (A20). Following the schema of Appendix A, we have

$$\tilde{S}_{hs}(r, k) = \tilde{S}_{hs0}(r, k) + \int_{R_1}^{R_0} dr_1 G_Q(r, r_1) \tilde{F}_{hs}(r_1, k), \tag{A23}$$

where $\tilde{S}_{hs0}(r, k)$ is solution of

$$\mathcal{D}_r \tilde{S}_{hs0}(r, k) = 0 \tag{A24}$$

which obeys the boundary conditions (A20), and $G_Q(r, r_1)$ is the Greens function of \mathcal{D}_r with the boundary condition

$$G_Q(r, r_1)|_{r=R_0} = 0, \quad G_Q(r, r_1)|_{r=R_1} = 0. \tag{A25}$$

We have

$$\tilde{S}_{hs0}(r, k) = (-1/r) C_S^{(-)}(k, \Delta p_1(R_0, k), p_0) + r C_S^{(+)}(k, \Delta p_1(R_0, k), p_0), \tag{A26}$$

where $C_S^{(-)}$ and $C_S^{(+)}$ are given by (85) and (86), respectively. $G_Q(r, r_1)$ is represented in terms of $\lambda_Q(m)$ and $\psi_Q(m, r)$ introduced by (67), (68) according to

$$G_Q(r, r_1) = \sum_{m=0}^{\infty} \psi_Q(m, r) r_1 \psi_Q(m, r_1) / \lambda_Q(m). \tag{A27}$$

Analogously to (A11), we expand $\tilde{S}_{hs0}(r, k)$ according to

$$\tilde{S}_{hs0}(r, k) = \sum_{m=0}^{\infty} \psi_Q(m, r) \beta_Q(m, k), \tag{A28}$$

$$\beta_Q(m, k) = \beta_Q^{(-)}(m) C_S^{(-)}(k, \Delta p_1(R_0, k), p_0) + \beta_Q^{(+)}(m) C_S^{(+)}(k, \Delta p_1(R_0, k), p_0), \tag{A29}$$

where $\beta_Q^{(-)}(m)$ and $\beta_Q^{(+)}(m)$ are given by (88).

Following the schema prescribed by (A11), (A12) and (A28), $\tilde{S}_{hs}(r, k)$ given by (A23) will be expanded according to

$$\tilde{S}_{hs}(r, k) = \sum_{m=0}^{\infty} \psi_Q(m, r) \tilde{S}_{2h}(m, k). \tag{A30}$$

Obviously, $\tilde{S}_{2h}(m, k)$ on the r. h. s. of (A30) always appears on the r. h. s. of (73), as concluded from (64), (71), and (73). Thus, $\tilde{S}_{2h}(m, k)$ is determined substituting (A30), (A21) and (A28) into (A23) and equating the coefficients of $\psi_Q(m, r)$. We get

$$\begin{aligned} \tilde{S}_{2h}(m, k) &= \beta_Q(m, k) + \left(1/\lambda_Q(m)\right) \int_{R_1}^{R_0} dr \psi_Q(m, r) r \tilde{F}_{hs}(r, k) \\ &= \beta_Q(m, k) + \tilde{S}_{2h}(m, k) \cdot (4\alpha^2 + 2k^2) / \lambda_Q(m) - (4\alpha^4 / \lambda_Q(m)) (d^2 / dk^2) \tilde{S}_{2h}(m, k), \end{aligned} \tag{A31}$$

which equals (76).

Appendix C

Arguments from the complex analysis will be used to show that (i) the Fourier-transformed hydrodynamic functions formally introduced in Section 3 satisfy the general preconditions as Fourier transforms, and (ii) belonging to a function class obeying further restrictive conditions. The Fourier-transformed equations of Section 3 appear as relationships within this function class only. The rearrangement of the hydrodynamic functions carried out in Section 3.4 will be taken as guide.

First, we estimate the analytic behavior of infinite sums with respect to n for $k \rightarrow \pm\infty$, occurring, e.g., in (108), and (110). As prototype, we consider

$$\sum_{n=0}^{\infty} \psi_A(n, r) \beta_A^{(1)}(n) \frac{\lambda_A(n)}{k^2 - \lambda_A(n)} = \sum_{n=0}^{\infty} \psi_A(n, r) \beta_A^{(1)}(n) \left(\frac{k^2}{k^2 - \lambda_A(n)} - 1 \right). \tag{A32}$$

(A32) is meromorphic in k with singularities on the imaginary k -axis only and holomorphic at least in the strip \mathcal{K} defined in Section 3.3. Regarding the second term in the bracket, the evaluation of the sum is elementary, applying (51), (52), and (47). To succeed with the first term, we conclude from (40), (41) that $\psi_A(0, r)$ is almost constant, meanwhile for $n \geq 1$, $\psi_A(n, r)$ which has n nodes for $R_1 \leq r \leq R_0$ can be approached by trigonometric functions, using the asymptotic representation of the cylinder functions which enter $\psi_A(n, r)$. Thus, we arrive at the estimations $|\psi_A(n, r) \beta_A^{(1)}(n)| < N_0$ for $n \geq 0$, and $-\lambda_A(n) > N_1 \cdot n^2$ for $n \geq 1$, where $N_0 > 0$, $N_1 > 0$ are appropriately chosen positive numbers ($N_1 \approx 100$). By contrast, $-\lambda_A(0) \approx 1.4$ is exceptional small compared with the other negative eigenvalues. After substitution of these estimations into (A32), the infinite sum can be evaluated in closed form. We arrive at (The Landau symbol O can be used to denote an estimated upper bound of the order for $k \rightarrow \pm\infty$, notwithstanding a lower-order behavior may occur in reality.)

$$\sum_{n=0}^{\infty} \psi_A(n, r) \beta_A^{(1)}(n) \frac{\lambda_A(n)}{k^2 - \lambda_A(n)} = O(k), \quad k \in \mathcal{K}, \quad k \rightarrow \pm\infty. \tag{A33}$$

There are further meromorphic functions of k involving infinite sums like (A32), also as holomorphic for $k \in \mathcal{K}$. Applying (A33), we find from (110), (49), and (50)

$$P_A(k) = \exp(-k^2/4\alpha^2) \cdot O(k^3), \quad k \in \mathcal{K}, \quad k \rightarrow \pm\infty, \tag{A34}$$

$$k^2 \tilde{A}_{\varphi h}^{(0)}(r, k) = \exp(-k^2/4\alpha^2) \cdot O(k^2), \quad k \in \mathcal{K}, \quad k \rightarrow \pm\infty, \tag{A35}$$

$$k^2 \tilde{A}_{\varphi h}^{(1)}(r, k) = O(k^2), \quad k \in \mathcal{K}, \quad k \rightarrow \pm\infty. \tag{A36}$$

Taking into account (113), (134), we have

$$k^2 \tilde{A}_{\varphi}^{(A)}(r, k) = \exp(-k^2/4\alpha^2) \cdot O(k^2), \quad k \in \mathcal{K}, \quad k \rightarrow \pm\infty, \tag{A37}$$

and together with (137), (139), and (141), we arrive at

$$\tilde{F}_2^{(A)}(m, k) = \exp(-k^2/2\alpha^2) \cdot O(k^4), \quad k \in \mathcal{K}, \quad k \rightarrow \pm\infty, \quad m = 0, 1, 2, \dots \tag{A38}$$

The functions (A34) to (A38) satisfy the preconditions to be Fourier transforms. In particular,

$$\int_{-\infty}^{\infty} dk |\tilde{F}_2^{(A)}(m, k)|^2 < \infty. \tag{A39}$$

(A39) is in turn the precondition that the solution $\tilde{S}_2^{(A)}(m, k)$ of (147), (149) is a Fourier transform, too, and represented as convergent series expansion in terms of $\psi_{S_2}(p, k)$ according to (151).

The overall consistency is proved showing that the hydrodynamic equations permit solutions of the vorticity function $\tilde{S}(r, k)$, to be holomorphic for $k \in \mathcal{K}$, and obeying

$$\tilde{S}(r, k) = \exp(-\beta k^2) \cdot O(k^p), \quad k \in \mathcal{K}, \quad k \rightarrow \pm\infty, \quad \beta > 0, \tag{A40}$$

with β and p to be determined later. If (A40) holds true, $\tilde{S}(r, k)$ is Fourier transform.

We start with the ad hoc presupposition that (A40) holds true. This also means that $\tilde{S}(r, k)$ with including the first and second k -derivative obey

$$|\tilde{S}(r, k)| < M_0, \quad |(\partial/\partial k)\tilde{S}(r, k)| < M_1, \quad |(\partial^2/\partial k^2)\tilde{S}(r, k)| < M_2, \quad k \in \mathcal{K}, \quad (\text{A41})$$

with appropriate positive bounds M_0, M_1, M_2 . Using the methods outlined here and in Section 3.4, we arrive at further estimations, namely from (109)

$$\mathcal{P}_S\{\tilde{S}\} = \exp(-\beta k^2) \cdot O(k^{p+1}), \quad k \in \mathcal{K}, \quad k \rightarrow \pm \infty, \quad (\text{A42})$$

so that from (107)

$$\Delta\tilde{p}_{1S}(R_0, k) = \exp(-\beta k^2) \cdot O(k^{p+1}), \quad k \in \mathcal{K}, \quad k \rightarrow \pm \infty. \quad (\text{A43})$$

In addition, we get from (55)

$$\tilde{A}_{\varphi p}(r, k) = \exp(-\beta k^2) \cdot O(k^{p-1}), \quad k \in \mathcal{K}, \quad k \rightarrow \pm \infty, \quad (\text{A44})$$

and from (135) together with (A36)

$$\tilde{A}_\varphi^{(S)}(r, k) = \exp(-\beta k^2) \cdot O(k^{p+1}), \quad k \in \mathcal{K}, \quad k \rightarrow \pm \infty. \quad (\text{A45})$$

Summarizing, we conclude from the initial presupposition (A40) that $\tilde{F}_2^{(S)}(m, k)$ given by (145) is holomorphic for $k \in \mathcal{K}$ and obeys

$$\tilde{F}_2^{(S)}(m, k) = \exp\left(-(\beta + 1/4\alpha^2)k^2\right) \cdot O(k^{p+5}), \quad k \in \mathcal{K}, \quad k \rightarrow \pm \infty. \quad (\text{A46})$$

We substitute $\tilde{S}(r, k)$ by $\tilde{S}_2(m, k)$ via (64) and (71) to (74). The functional dependence upon $\tilde{S}_2(m, k)$ may be underlined writing

$$\tilde{F}_2^{(S)}(m, k) = \tilde{F}_2^{(S_2)}(m, k, \{\tilde{S}_2\}). \quad (\text{A47})$$

The result of this section can be rewritten as follows: If (A37) holds true, and $\tilde{S}_2(m, k)$ obeys

$$\tilde{S}_2(m, k) = \exp(-\beta_2 k^2) \cdot O(k^p), \quad k \in \mathcal{K}, \quad k \rightarrow \pm \infty, \quad \beta_2 > 0, \quad (\text{A48})$$

then (A46) is holomorphic for $k \in \mathcal{K}$, and (A43) becomes

$$\tilde{F}_2^{(S_2)}(m, k, \{\tilde{S}_2\}) = \exp(-\beta_2 k^2) \cdot O(k^{p+5}), \quad k \in \mathcal{K}, \quad k \rightarrow \pm \infty. \quad (\text{A49})$$

We again discuss the differential Equation (80). We split $\tilde{F}_2(m, k)$ on the r. h. s. according to (143)

$$\tilde{F}_2(m, k) = \tilde{F}_2^{(A)}(m, k) + \tilde{F}_2^{(S_2)}(m, k, \{\tilde{S}_2\}). \quad (\text{A50})$$

(80) is a system of implicit, linear differential equations where second-order derivatives of $\tilde{S}_2(m, k)$ appear on the r. h. s., as seen from (83) together with (55). Considered to be a linear algebraic equation system for $(d^2/dk^2)\tilde{S}_2(m, k)$, this system is regularly resolved for $(d^2/dk^2)\tilde{S}_2(m, k)$, near the real k -axis, to become the normal form of explicit second-order systems of differential equations with holomorphic coefficients for $|\Im k| < a$ (see the definition of \mathcal{K} in Section 3.4). For the parameter area considered in our work, we find $a \approx 0.4 < \sqrt{|\lambda_A(0)|}$. This provided, it is concluded from fundamental theorems on local, regular, and analytic solutions of ordinary differential equations and their analytic continuation [34] that, say around $k = 0$, the equation system (80) is solved for holomorphic solutions $\tilde{S}_2(m, k)$ only, which can be analytically continued for all k with $k \in \mathcal{K}$. This

approach is found again in the self-consistent determination of the vorticity function discussed in Section 3.4.

The consistency is finally verified showing that $\tilde{S}_2(m, k)$, considered to be particular solution of (80), belongs to the function class characterized by (A48). Provided (A48) holds true, we determine β_2 and p by comparison of the leading order in (80) for $k \in \mathcal{K}$, $k \rightarrow \pm\infty$, substituting (A50), (A38) and (A46) on the r. h. s. of (80) and using

$$\mathcal{L}(m)\tilde{S}_2(m, k) = \exp(-\beta_2 k^2) \cdot O(k^{p+2}), \quad k \in \mathcal{K}, \quad k \rightarrow \pm\infty. \tag{A51}$$

We arrive at $\beta_2 = 1/2\alpha$, $p + 5 = 4$, so that

$$\tilde{S}_2(m, k) = \exp(-k^2/2\alpha^2) \cdot O(1/k), \quad k \in \mathcal{K}, \quad k \rightarrow \pm\infty, \tag{A52}$$

and from (73) and (74)

$$\tilde{S}(r, k) = \exp(-k^2/4\alpha^2) \cdot O(1/k), \quad k \in \mathcal{K}, \quad k \rightarrow \pm\infty, \tag{A53}$$

We note that according to (A53), $\tilde{S}(r, k)$ stronger decreases for $k \rightarrow \pm\infty$ than predicted by the truncated series expansion (99).

Appendix D. Analytic Fit of Fac($R_1/R_0, \alpha$)

For $0.60 \leq R_1/R_0 \leq 0.95$ and $0 \leq \alpha \leq 3$, the correction factor Fac($R_1/R_0, \alpha$) is given by the analytic approximant

$$\text{Fac}(R_1/R_0, \alpha) = \frac{1}{1 + c_2\alpha^2 + c_4\alpha^4 + c_6\alpha^6}$$

with an accuracy better than $\pm 1 \cdot 10^{-3}$.

Table A1. Coefficients of Fac($R_1/R_0, \alpha$).

R_1/R_0	c_2	c_4	c_6
0.60	0.06641	0.02852	-0.00145
0.70	0.06084	0.02658	-0.00117
0.80	0.05805	0.01776	-0.00056
0.90	0.06280	0.00498	0.00000
0.95	0.06358	0.00164	-0.00001

Appendix E. List of Recurring Mathematical Symbols Used in Several Paragraphs

The number behind denotes the equation number where the symbol is defined or explained in the corresponding text. The tilde to indicate Fourier transforms is neglected. No distinction is made between dimensionless quantities and quantities with a dimension. Arguments are not explained (see text).

- \mathbf{A} (9), A_φ (10), $A_{\varphi h}$, $A_{\varphi p}$ (25), $A_{\varphi h}^{(0)}$, $A_{\varphi h}^{(1)}$ (48), $A_\varphi^{(A)}$ (134), $A_\varphi^{(S)}$ (135), $A_\varphi^{(SE)}$ (154), C_A^+ (45), C_A^- (46), C_S^+ (85), C_S^- (86), \mathcal{D}_r (16), *Erhy* (199), *Fac* (187), F_h , F_p , F_2 , F_{2h} (82), $F_{2h}^{(A)}$, $F_{2h}^{(S)}$ (139), $F_{hp}^{(SA)}$, $F_{hp}^{(S)}$ (158), $F_2^{(A)}$, $F_2^{(S)}$ (143), $F_{2h}^{(SE)}$ (157), $F_{hp}^{(A)}$, $F_{hp}^{(S)}$ (140), $F_{hp}^{(S)}$ (158), $F_{hp}^{(SE)}$ (159), f_2 (96), $f_2^{(A)}$ (160), $f_2^{(SE)}$ (165), \mathcal{L} (78), p (1), p_0 , Δp (21), Δp_1 (35), p_T , p_h (190), Δp_{1A} , Δp_{1S} (105), P_A (110), \mathcal{P}_1 (108), \mathcal{P}_S (109), r , R_0 , R_1 (1), ΔR_0 (177), S (17), S_h , S_p (64), S_{2h} (73), S_{2p} (74), $S_2^{(A)}$ (146), $S_2^{(S)}$ (147), S_{m_1, p_1} (99), s_2 (97), $s_2^{(A)}$ (151), $s_2^{(S)}$ (167), u (174), \mathbf{v} (1), v_r (11), v_T (7), v_z (12), v_{rh} (27), W (189), ΔW (178), w (179), z (1), Δz_e (6), α (8), β_A (43), β_A^- , β_A^+ (47), $\beta_A^{(0)}$, $\beta_A^{(1)}$ (51), β_Q^- , β_Q^+ (88),

$$\begin{aligned} &\eta \text{ (1)}, \eta_{min} \text{ (6)}, \lambda_A \text{ (40)}, \lambda_Q \text{ (68)}, \lambda_{S2} \text{ (94)}, \\ &\sigma' \text{ (1)}, \sigma'_{rr} \text{ (19)}, \sigma'_{rz} \text{ (20)}, \tau \text{ (8)}, \\ &\psi \text{ (95)}, \psi_A \text{ (39)}, \psi_Q \text{ (68)}, \psi_{S2} \text{ (93)}, \psi_{PA} \text{ (114)}, \psi_{PS} \text{ (121)}, \\ &\Phi \text{ (87)}, \Phi^{(A)} \text{ (137)}, \Phi^{(S)} \text{ (138)}, \Phi^{(SE)} \text{ (156)} \end{aligned}$$

References

- Lewis, J.A. The collapse of a viscous tube. *J. Fluid Mech.* **1977**, *81*, 129–135. [[CrossRef](#)]
- Kirchhof, J. A hydrodynamic theory of the collapsing process for the preparation of optical waveguide preforms. *Phys. Status Solidi (a)* **1980**, *60*, K127–K131. [[CrossRef](#)]
- Kirchhof, J. Reactor problems in modified chemical vapour deposition (I). The collapse of quartz tubes. *Cryst. Res. Technol.* **1985**, *20*, 705–712. [[CrossRef](#)]
- Kirchhof, J.; Funke, A. Reactor problems in modified chemical vapour deposition (II). The mean viscosity of quartz glass reactor tubes. *Cryst. Res. Technol.* **1986**, *21*, 763–770. [[CrossRef](#)]
- Geyling, F.T.; Walker, K.L.; Csencsits, R. The viscous collapse of thick-walled tubes. *J. Appl. Mech.* **1983**, *50*, 303–310. [[CrossRef](#)]
- Das, S.K.; Gandhi, K.S. A model for thermal collapse of tubes. Application for optical glass fibres. *Chem. Eng. Sci.* **1986**, *41*, 73–81. [[CrossRef](#)]
- Yarin, A.L.; Bernat, V.; Doupovec, J.; Miklos, P. The viscous collapse of radial nonsymmetric composite tubes. *J. Light. Technol.* **1993**, *11*, 198–204. [[CrossRef](#)]
- Makovetskii, A.A.; Zamyatin, A.A.; Ivanov, G.A. Technique for estimating the viscosity of molten silica glass on the kinetics of the collapse of the glass capillary. *Glass Phys. Chem.* **2014**, *40*, 526–530. [[CrossRef](#)]
- Kirchhof, J.; Unger, S. Viscous behavior of synthetic silica glass tubes during collapsing. *Opt. Mater. Express* **2017**, *7*, 386–400. [[CrossRef](#)]
- Kirchhof, J.; Unger, S.; Dellith, J. Viscosity of fluorine-doped silica glasses. *Opt. Mater. Express* **2018**, *8*, 2559–2569. [[CrossRef](#)]
- Klupsch, T.; Pan, Z. Collapsing of glass tubes: Analytic approaches in a hydrodynamic problem with free boundaries. *J. Eng. Math.* **2017**, *106*, 143–168. [[CrossRef](#)]
- Fitt, A.D.; Furusawa, K.; Monro, T.M.; Please, C.P. Modelling of the fabrication of hollow fibers: Capillary drawing. *J. Lightwave Technol.* **2001**, *19*, 1924–1931. [[CrossRef](#)]
- Fitt, A.D.; Furusawa, K.; Monro, T.M.; Please, C.P.; Richardson D.J. The mathematical modeling of capillary drawing for holey fibre manufacture. *J. Eng. Math.* **2002**, *43*, 201–227. [[CrossRef](#)]
- Kostecki, R.; Ebendorff-Heidepriem, H.; Warren-Smith, S.C.; Monro, T.M. Predicting the drawing conditions for microstructured optical fiber fabrication. *Opt. Mater. Express* **2014**, *4*, 29–40. [[CrossRef](#)]
- Stokes, Y.M.; Buchak, P.; Crowdy, D.G.; Ebendorff-Heidepriem, H. Drawing of microstructured fibres: Circular and non-circular tubes. *J. Fluid Mech.* **2014**, *755*, 176–203. [[CrossRef](#)]
- Buchak, P.; Crowdy, D.C.; Stokes, Y.M.; Ebendorff-Heidepriem, H. Elliptical pore regularization of the inverse problem of microstructured optical fibre fabrication. *J. Fluid Mech.* **2015**, *778*, 5–38. [[CrossRef](#)]
- Chen, M.J.; Stokes, Y.M.; Buchak, P.; Crowdy, D.C.; Ebendorff-Heidepriem, H. Microstructured optical fibre drawing with active channel pressurization. *J. Fluid Mech.* **2015**, *783*, 137–165. [[CrossRef](#)]
- O’Kiely, D.; Breward, C.J.W.; Griffiths, I.M.; Howell, P.D. Edge behavior in the glass sheet redraw process. *J. Fluid Mech.* **2015**, *785*, 248–269.
- Marquis, S.G.; O’Kiely, D.; Howell, P.D.; Lange, U.; Griffiths, I.M. Response to periodic disturbances in the glass redraw process. *J. Eng. Math.* **2020**, *121*, 39–56. [[CrossRef](#)]
- Boyd, K.; Ebendorff-Heidepriem, H.; Monro, T.M.; Munch, J. Surface tension and viscosity measurement of optical glasses using a scanning CO₂ laser. *Opt. Mater. Express* **2012**, *2*, 1101–1110. [[CrossRef](#)]
- Scholze, H. *Glass: Nature, Structure, and Properties*; Springer: New York, NY, USA, 1990.
- Parmelee, C.W.; Lyon, K.L.; Harman, C.G. The surface tensions of molten glass. In *Engineering Experiment Station, Bulletin Series No. 311*; University of Illinois: Urbana, IL, USA, 1939.
- Peak U.C.; Bunk, R.B. Physical behavior of the neck-down region during furnace drawing of silica fibers. *J. Appl. Phys.* **1978**, *48*, 4417–4422. [[CrossRef](#)]
- Martin, M.H. The flow of a viscous fluid. *Rat. Mech. Anal.* **1971**, *41*, 266–287. [[CrossRef](#)]
- Naeem, R.K.; Ali, S.A. A class of exact solutions to equations governing the steady state flows of an incompressible fluid of variable viscosity via von Mises variables. *Int. J. Appl. Mech. Eng.* **2001**, *6*, 395–426.
- Naeem, R.K.; Jamil, M. On plane steady flows of an incompressible fluid with variable viscosity. *Int. J. Appl. Math. Mech.* **2006**, *2*, 1–19.
- Naaem, K.N.; Mansoor, A.; Khan, W.A. Aurangzaib, Exact solutions of steady plane flows of an incompressible fluid of variable viscosity using (ξ, ψ) - or (η, ψ) -coordinates. *World Acad. Sci. Eng. Technol.* **2009**, *35*, 1022–1028
- Zhong, S. Analytic solutions for Stokes flow with lateral variations in viscosity. *Geophys. J. Int.* **1996**, *124*, 18–28. [[CrossRef](#)]
- Fatsis, A.; Statharas, J.; Panoutsopoulou, A.; Vlachakis, N. On the exact solution of incompressible viscous flows with variable viscosity. *WIT Trans. Eng. Sci.* **2012**, *74*, 481–492.
- Popov, Y.I.; Lobanov, I.S.; Popov, S.I.; Popov, A.I.; Gerya, T.V. Practical analytical solutions for benchmarking of 2-D and 3-D geodynamic Stokes problems with variable viscosity. *Solid Earth Discuss.* **2013**, *5*, 2203–2281.

-
31. Popov, I.Y.; Makeev, I.; Blinova, I.V. Analytical benchmark solutions for Stokes flow with variable viscosity in spherical layer. *Progr. Comp. Fluid Dyn.* **2018**, *18*, 56–68. [[CrossRef](#)]
 32. Sommerfeld, A. *Vorlesungen über Theoretische Physik. Band II: Mechanik der Deformierbaren Medien*; Akademische Verlagsgesellschaft Geest und Portig: Leipzig, Germany, 1970.
 33. Fischer, H.; Kaul, H. *Mathematik für Physiker, Band 2: Gewöhnliche und Partielle Differentialgleichungen, Mathematische Grundlagen der Quantenmechanik*; Teubner: Wiesbaden, Germany, 2008.
 34. Bieberbach, L. *Theorie der gewöhnlichen Differentialgleichungen, auf Funktionentheoretischer Grundlage Dargestellt*; Springer: Berlin, Germany, 1953.